German-Dutch Wind Tunnels

Annual Report 2007

Duits-Nederlandse Windtunnels

Deutsch-Niederländische Windkanäle

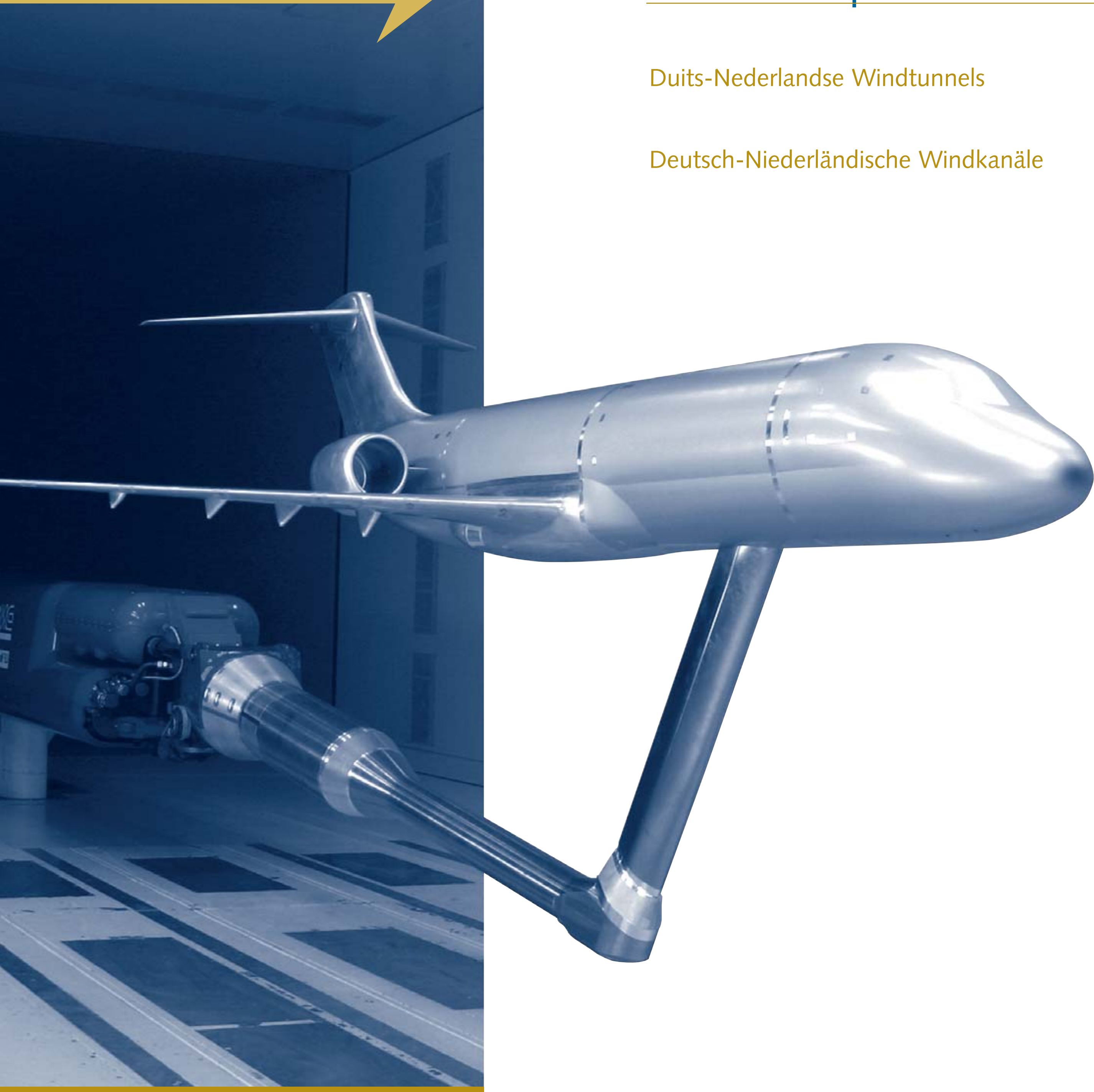

German-Dutch Wind Tunnels

MAIL

DNW
P.O. Box 175
8300 AD Emmeloord
The Netherlands

E-MAIL

info@dnw.aero

WEB

www.dnw.aero

PHONE

Exchange:	+31 527 24 8555
Central office:	+31 527 24 8520

FAX

+31 527 24 8582

The Foundation DNW has been established by Deutsches Zentrum für Luft- und Raumfahrt e.V. (DLR) and Stichting Nationaal Lucht- en Ruimtevaartlaboratorium (NLR).

Contents

German-Dutch Wind Tunnels

Preface

Every year DNW produces an Annual Report in which some of the more significant projects and the new levels of technology attained in the technical status of our facilities are reported on. The reporting is performed by the colleagues from amongst the user community of our wind tunnels as well as us. The contributions from the user community come either in the form of a full report or various inputs or comments sufficient for DNW to make a report or sometimes the granting of permission to use the information from their project in our own reporting. All forms of contributions are sincerely appreciated. These contributions are appreciated not only for the sake of the work that goes into the preparation of a chapter to be included within the context of the DNW Annual Report. They are especially appreciated for their meaning to the DNW, for their providing of evidence that our goals are strongly intertwined with the goals and progress of our user community.

Our user community consists to a large extent of companies engaged in the development and production of flying vehicles; ground vehicles constitute a smaller proportion of the aerodynamic experimentation in our wind tunnels. Another component of the usage of our wind tunnels originates in research. What is common to these sectors, researchers and product developers, is their drive to be the best in their chosen field. Just as the researchers strive to create new understanding, and to shift the boundaries of knowledge, the product developers are striving to develop products that are more competitive than the previous generation of the products available on the world market. It seems obvious that those goals are directly compatible with the Lisbon Agenda of the European Union, where the goal of achieving the status of the most competitive economy was adopted for Europe. How else, than by applying new knowledge to the creation of competitive products, does one obtain a competitive economy?

Just like our user community, DNW is engaged in shifting the boundaries of experimental aerodynamic simulation, with the goal of providing the best research infrastructure and service in the world. DNW is committed to the concept of competitive test services worldwide while maintaining the coverage of its strategic position in Europe. Just like the national laboratories overseas (in the US, China, etc.) provide strategic capability for national needs, the DNW is dedicated to providing its share of the strategic capabilities within Europe. Although DNW is not in a similarly favorable position as the NASA wind tunnels with their large institutional funding, it has been possible to maintain our leading edge worldwide as evidenced by the mix of project highlights in the current Annual Report. The competitive position of DNW is the result of the enthusiasm and dedication of our employees, but also of the support of our parent institutions (DLR-Germany and NLR-The Netherlands) that have over the years enabled DNW to improve its available infrastructure. Both the enthusiasm and the support are reinforced by the positive global response to the skills and capabilities of DNW, and the success of the European aeronautical industry in the global market. In its efforts to provide infrastructure support to the European research and development effort, DNW is complementary to the strategy of the EU. Befittingly, DNW is working to establish itself as an organization worthy of infrastructure support not only of its host countries, but from the European Commission as well. This way Europe will continue to be able to rely on having an independent and competitive technological basis, for the good of the global benefits of mobility and transportation. DNW is willing to carry its share of this responsibility.

German-Dutch Wind Tunnels

Occupation of Facilities - Status and Prospects

Although the year 2007 was not another record year for DNW - it was just another busy year – it exhibited a familiar pattern, where the heaviest product development related workload was again concentrated in the low-speed wind tunnel LLF. As in previous years, this Annual Report gives an account of a number of significant projects in the chapter "Highlights of Project Work". The current overview of occupational patterns and status discusses the situation and presents a number of general observations, including that of the repeated occurrence of the non-uniform occupational patterns across the entire range of capabilities offered by DNW.

The requirements toward the capabilities and know-how of the DNW staff persevered in a manner similar to preceding years. Tests for the development of propeller aircraft continued in the LLF for both large customers of the previous year. Both the EADS A400M project, as well as the US Naval Air Command E-2D Hawkeye project, continued to verify their new designs in our wind tunnel. Both projects were critically relying upon the existence and availability in the DNW of the necessary know-how for propeller aircraft simulation in wind tunnels. The complexity of testing a model with air-driven propeller engines, accounting for the added acceleration of the airflow due to the driven propellers and the need to apply appropriate correction procedures to obtain interference-free results, were just the sort of challenge that brought out the best characteristics of the DNW.

The ambitious goal of the Chinese authorities represented by the First Aircraft Institute (FAI) of AVIC 1, to become a major producer of commercial civil transport aircraft, was reflected in the occupation of DNW wind tunnels as well. Although DNW had tested on behalf of the Chinese development programs before, in 2007 the amount of testing grew, and also became more product-oriented (as opposed to phenomenon-oriented pre-development testing), with test entries taking place in both large wind tunnels of DNW, the LLF and the HST. In addition to the above mentioned regional jet aircraft development, the HST maintained its steady place in the development programs of manufacturers of business jet aircraft. This tunnel is just of the appropriate size for that class of aircraft. The scaling down is not excessive for smaller aircraft so that sufficient detail can be represented at model scale. Israel Aerospace Industries can be mentioned as a representative customer from this market segment.

As in almost every year, some rotary wing testing took place and provided challenging experiments. In 2007 the EU sponsored research project studying the tilt-rotor aircraft, ADYN, used DNW's facilities and infrastructure for studying the flow/structure interaction phenomenon, called whirl flutter. This test was a continuation of the European effort at establishing the know-how necessary for successful development of tilt-rotor aircraft, with participation coming from the research community, national laboratories, and the relevant industry.

Some more testing for the fighter aircraft EFA Typhoon II (see Figure 1) took place in the DNW wind tunnels, confirming the need of even relatively mature projects to utilize aerodynamic experimental simulation for novel applications in the project.

In a continuous stream, testing for ground-based vehicle development challenges the capabilities of DNW. Both high Reynolds number facilities, the KKK and HDG, were utilized for train simulations, while the NWB and LLF were used for heavy truck testing by MAN. In train testing, the simulation of the interaction between crosswinds, the vehicle and the ground structure such as an embankment or bridge, still poses some unresolved challenges to the vehicle developers.

Another significant and highly visible area of expertise in DNW remains the portfolio of high-quality simulations of dynamic phenomena. We continued to utilize NWB's Model Positioning Mechanism (MPM), providing a unique maneuver simulation capability both for developmental and research customers. This capacity, unique in its quality and flexibility, which was developed with the support of DLR research, has now reached a level of maturity that makes it an indispensable tool for industrial developments.

As in the previous year, a considerable share of the demand for high-speed testing was provided by missile developments. In this situation, having some partially redundant capacity within one organization proved to be crucial to satisfying the experimental simulation needs of our customers. As the TWG ceased to be available to the user community due to the fatigue in its old compressor blades, the customers' tests were switched into the HST without any loss of schedule or simulation range. Thus, the missile testing domain maintains its strong presence in DNW's capabilities portfolio despite the temporary shutdown of one of our key facilities.

As formulated in the previous year, the range of capabilities within DNW ensures that weaknesses in one market segment can be compensated by the strength in another, if the market develops at different rates in different segments. There have to be growth segments to compensate for the shrinking segments, though. During the last few years DNW's operations have owed their success to the strength in low-speed testing, primarily coupled with the simulation of ground effects for both fixed wing transport aircraft configurations as well as fighter configurations. The capability of simulating engine integration effects in ground proximity is expected to continue providing the bulk of testing volume into the following year, but not at the same intensity any more. There are no large new fighter aircraft programs on the horizon. Also, since the largest industrial tunnel of DNW, the LLF, obtains most of its high-intensity tests in the later phases of a development program, the new post-A380 European projects will start appearing in DNW's planning after a few years of delay.

Newly emerging aircraft development programs from countries such as China, are expected to make use of the established strengths of DNW and will contribute to the occupancy of our industrial tunnels LLF and HST. The Chinese ARJ21 program has grown beyond the use of the HST; it is also utilizing the engine integration simulation capabilities of the LLF.

The research market can be expected to remain stable, providing occupancy mainly in the smaller tunnels operated by DNW. The large EU-sponsored research programs still largely bypass DNW, as the priority seems to remain in establishing and supporting the capability provided by ETW. The exception to this trend is formed by the rotary wing aircraft community, including that for tilt-rotor aircraft. This community has no alternative for the

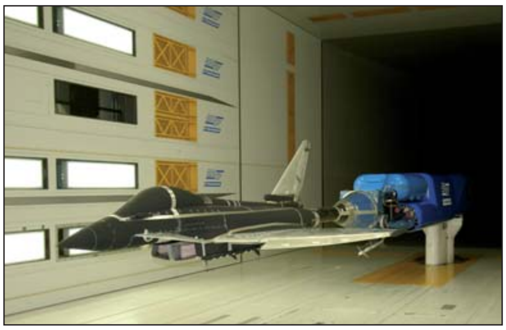

Figure 1: EFA Typhoon II model in the LLF

German-Dutch Wind Tunnels

scale advantages provided by the two large European wind tunnels, the DNW-LLF for low-speed testing and the S1 of ONERA-GMT for high-speed testing. Consequently, a regular stream of testing of moderate intensity will continue.

The US is the major non-European market for DNW's testing services. In this context, the JSF has already been mentioned in previous Annual Reports, along with the testing for the E-2D Hawkeye under contract to US Naval Air Command. These two aircraft programs bear witness to the quality of DNW's facilities and team, and they provide a basis for further activities in this market. On the other hand, in a number of studies performed for the US defense agencies, DNW has been identified as a major competitor, even as a threat to the national facilities. This has triggered funding for extra government support for NASA-operated test facilities. This in turn has made it significantly more difficult to attract customers from the US, since the institutionally funded facilities don't rely on recovering their costs from the customers to stay operational.

Overall, on the background of past experience and the developments in the aerospace world, the following year (2008) can be anticipated to be a year with fewer large industrial development projects than in previous years for the DNW as a whole. At the same time, this development will permit the planning of urgently required maintenance and upgrading activities, which have suffered in their priority in recent years due to maximum tunnel utilization. This planning, together with DNW's response capability to re-allocate resources in response to outside developments, ensure DNW remains fully operational, and continues to provide all the testing services its customers have come to expect from DNW.

Photographs released by courtesy of Gulfstream and EADS-CASA.

Highlights of Project Work

Fixed Wing Civil Transport Aircraft

Investigations of the Advanced Regional Aircraft ARJ21

During the development of the Advanced Regional Jet (ARJ21) for the 21st century, extensive wind tunnel tests on scaled models of this aircraft were performed in both, the DNW-LLF as well as the DNW–HST. The ARJ21 is under development by the Chinese First Aircraft Institute (FAI) of AVIC1. The performance of this aircraft has to meet the diverse and demanding operating conditions found in China, including hot and high altitude conditions. Therefore, the aircraft needs a powerful take-off and climbing performance to allow it to use basic airports with short runways.

The ARJ21 is a regional jet aircraft with a low wing and powered by two General Electric CF34-10A engines, mounted on the rear fuselage, forward of the swept T-tail. It will carry 70 to 80 passengers. In December 2007, the roll-out of the first ARJ21-700 took place (see photograph above). The maiden flight of the ARJ21 is due in 2008 and the first aircraft will be delivered to customers in 2009, after receiving its airworthiness certificate earlier that year.

For testing the laminar supercritical wing configuration around the cruise condition, FAI selected the HST 2 m x 1.8 m test section. This investigation was performed using a new 1:20 scale ARJ21-700 model, with a wing span and a length of 1.33 m and 1.67 m, respectively. The model was designed and manufactured by FAI. This new model differed from the previous model that was tested in the HST in 2004 (see Annual Report 2004). The main differences were an extension to the fuselage length and the modifications to the wing geometry. The model was mounted on a Z-sting support for longitudinal measurements and the double roll boom support for lateral measurements. Overall model forces and moments were measured with an internal 2.5″ TASK balance.

The tests were performed at Mach numbers ranging between 0.2 and 0.82. The main objectives of the test were:

- To obtain the basic longitudinal/lateral aerodynamic characteristics of the aircraft as a function of Mach number at a constant high Reynolds number
- To obtain the efficiency of the control surfaces such as horizontal tailplane, ailerons, elevators, rudder and spoilers, as a function of Mach number at a constant Reynolds number
- To locate the position of laminar-turbulent boundary-layer transition on the lifting surfaces, nacelles and fuselage
- Detailed flow visualization by means of colored oil applied to the model surface to observe the surface flow characteristics

Figure 1: Guests from China inspect the small-scale ARJ21 model mounted inverted in the HST for ground interference assessments

Figure 2: ARJ21 large-scale model mounted in the LLF with a ventral sting setup

Figure 3: ARJ21 large-scale model mounted in the LLF above the ground plane with a dorsal sting setup

Special attention was given to the laminar wing design. The main part of the test was performed without tripping the boundary layer on the model parts (wing, fuselage, etc.). The test repeatability was still excellent, despite having free transition of the boundary layer on the model surfaces.

Apart from the measurements of the aircraft performance and surface flows for the aircraft performance database, extensive support interference measurements were made as well (see Figure 1). The state-of-the-art sting interference correction procedure for the HST is presented as the next highlight in this report.

The aircraft's take-off and landing performances were measured in the LLF 8 m x 6 m test section. For these tests, FAI designed and manufactured a 1:5.8 scale model, with a wing span and a length of 4.6 m and 5.2 m, respectively. The model was provided with the internal W608 balance for measurement of the overall model forces and moments. The control surfaces, such as horizontal tailplane, elevators, rudder and ailerons, were remotely controlled to increase the test productivity. A productivity increase of about 30% was achieved. The remote control equipment (motors, etc.) was supplied by DNW.
The test matrix consisted of conditions simulating free flight and ground effect. For the free flight tests, the ventral sting setup was used and the model was located on the tunnel center-line (see Figure 2). For the ground effect tests the dorsal sting setup was used (see Figure 3), which allowed the model's height above the ground to be varied. With both setups the longitudinal and lateral movements were achieved using the sting support mechanism. During the ground effect testing, a ground plane was used, with an upstream scoop as a boundary layer control device. The upper flow surface of the ground plane was 0.2 m higher than the test section floor. In this way the tunnel floor boundary layer that forms upstream of the test section was removed. Instead of using the conventional moving belt, non-moving type polyester sheets were chosen and taped to the floor. Due to the high location of the engines the thin new boundary layer, which developed on the ground plane, was found to have no impact on the test results.

The tests were performed at Mach number 0.2 (equivalent to a wind speed of 70 m/s). The main objectives of the test in free flight and ground effect were:

- To obtain the basic longitudinal/lateral aerodynamic characteristics of the aircraft in cruise, take-off and landing configurations
- To test the efficiency of the control surfaces such as horizontal tail, ailerons, elevators, rudder and spoilers in cruise, take-off and landing configuration

Again, free transition of the boundary layer on the model surfaces was used. As for the high-speed testing, the test repeatability was also excellent at low speeds.

Apart from the above mentioned database measurements of the aircraft performance, extensive support interference measurements were made (see Figure 4). The sting interference correction procedure applied is standard at the LLF and has already been described in or Annual Report 2004.

During both the HST and LLF tests, the engines of the aircraft were represented on the model by the so-called through flow nacelles (see Figure 5). In 2008, a test of the same 1:5.8 scale model fitted with Turbofan Propulsion Simulator (TPS) units is planned in the LLF. The engine air-intake and exhaust flows will be simulated by TPS units with 9″ intake diameters. The model has already been prepared and fitted with a high pressure air feed for the TPS units.

We are confident that also these tests will also become a success we can report in our next Annual Report.

Photographs released by courtesy of FAI AVIC1

Figure 4: ARJ21 large-scale model in the LLF on a ventral sting and fitted with a dummy dorsal sting for support interference assessment

Figure 5: Through-flow nacelle fitted to the ARJ21 large-scale model

German-Dutch Wind Tunnels

Towards a New Support Interference Approach in the DNW-HST

Introduction

Since 2003, several wind tunnel test campaigns have been conducted on behalf of Israel Aerospace Industries (IAI). Tests were performed for several business jet models that were developed by IAI. For test efficiency reasons, a model support boom was chosen with pitch and sideslip capabilities over a wide operational range. The drawback to this choice of test setup was the relatively large support interference effect generated. Until quite recently, the wind tunnel results for these tests were only corrected in drag for the support interference of the boom. The correction was based on the buoyancy effect of the chosen boom using a dedicated empty test section pressure distribution.

Due to the relatively large correction on drag that was required, as well as the lack of corrections for lift and pitching moment, IAI and DNW agreed to perform a dedicated support interference test. The main goal of the test was to obtain the support interferences on drag, lift and pitching moment. In addition to that a validation of the standard buoyancy correction was desired. The test has resulted in an updated support interference approach for testing in the HST.

Approach

Experimental

In the common support interference approach of the HST, the interference contributions are differentiated in so-called far- and near-field effects (see Figure 1).

The far-field interference gives an overall tunnel flow field disturbance due to the presence of the model support boom in the wind tunnel. In the common approach, it is considered sufficient to correct for this disturbance by buoyancy corrections on drag only. No correction for lift and pitching moment are applied.

The near-field contribution is related to the direct effect of the sting on the flow around the model itself. This effect results in a change of the local pressure field and boundary layer where the sting enters into the model. In addition, a change of local flow direction might result, due to the presence of the sting. This may accrue in quite significant effects on lift and pitching moment as well, when lifting surfaces are close by. Near-field corrections are usually applied to lift, drag and pitching moment.

In the common approach, the near-field effects are obtained by mounting the model on an alternative support setup and placing a dummy original sting close to the model. The effect of the original sting is determined from the difference in aerodynamic coefficients obtained with and without the dummy sting present. The common approach was earlier described in Annual Report 2004 in relation to the development of the Chinese ARJ21 aircraft.

As an extension to the common approach, the far-field effects are also derived from dedicated interference measurements. The far field-effects are determined from the difference in aerodynamic coefficients between runs with and without the boom.
The far-field effects were compared with the standard buoyancy corrections for drag. By combining the effects of near- and far-field, the total support interference is obtained.

Numerical

On behalf of DNW, the National Aerospace Laboratory (NLR) has conducted Computational Fluid Dynamics (CFD) calculations of the model and support configurations that were investigated experimentally. The goal of this work was to investigate whether CFD might be a suitable tool for validation of the extended experimental approach. In addition to this, it was investigated whether CFD has potential to replace these kinds of experiments completely, considering the quality, time and cost involved.

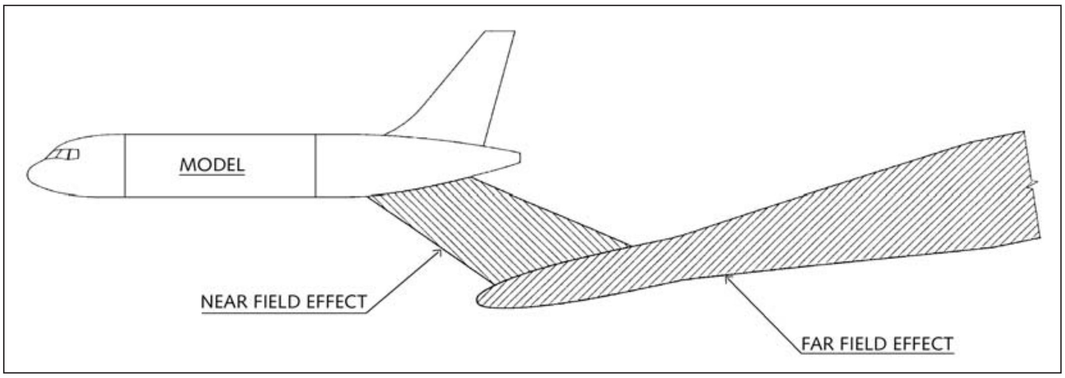

Figure 1: Schematic identification of the sources of near- and far-field support interference contributions

Two approaches were followed:

1. Calculations for an IAI business jet model with and without the model support elements in an infinite flow field.
2. Calculations for an IAI business jet model with and without the model support elements including the presence of the tunnel walls and dorsal sting. In this approach, the experimental setups were simulated completely in the CFD.

From a cost and time efficiency point of view, the first approach is preferable over the second approach. However, from a quality point of view it was not clear, which of the two approaches gave the better results. Hence, both approaches were adopted.

The flow calculations were performed using the NLR flow simulation solver "ENFLOW" for multi-block structured flow domains. The selected aerodynamic model in this study was the full Reynolds-Averaged Navier Stokes (RANS) model to include important viscous effects.

Wind tunnel model and test setup

Force and moments measurements were performed with an internal balance for two business jet models. The models were mounted upside down on a dorsal sting (see Figure 2) in order to minimize mutual interference between the dorsal sting and the dummy support.

The original production runs were performed using the articulated boom support and a Z-sting. In order to determine the interference effects of the support, a dummy Z-sting was mounted on the articulated boom support. The dummy Z-sting blade penetrated the model's aft-body. Care was taken to avoid any contact between the dummy sting and the model. The lower side of the dummy blade was made of a rubber material in order to prevent balance damage in the unlikely event the dummy blade touched the model.

For accurate measurements, it was necessary to align the dummy support in the same position with respect to the model, as during the original production runs. Consequently, the dorsal sting was mounted on a horizontal traversing slide to compensate for differences in horizontal alignment (between the model and the dummy support) at different model angles-of-attack.

Pressure transducers were mounted in the aft-body cavity in order to monitor any simulation differences between the production and support interference runs. The differences were found to be negligible.

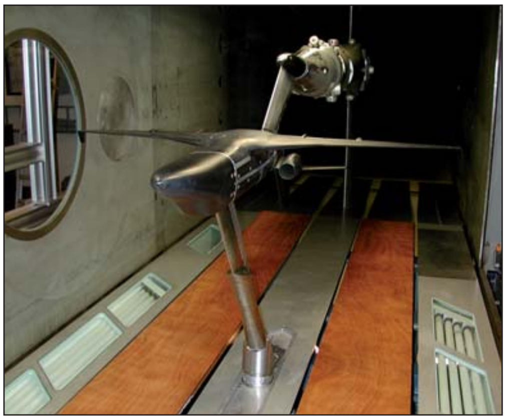

Figure 2: Test setup for support interference investigations with an IAI business jet model mounted upside down on a dorsal sting in the HST

Test program

These experiments were performed in the Summer of 2007. Measurements were performed over a Mach number range of 0.24 to 0.9 and an angle-of-attack range of -2° to +5°. A Reynolds number of 4.5 million was maintained throughout the test. In order to investigate the effects of the support on the model's tail, measurements were conducted for tail-on and tail-off configurations.

A pitch and pause procedure was necessary for the configurations with the dummy Z-sting, to prevent any contact between the sting and the model. The configurations with the dummy boom support also required a pitch and pause procedure in order to position the boom at the same locations as used during the runs with the dummy Z-sting. The configurations without the dummy support were measured in a continuous sweep, as for the production runs.

The CFD calculations were performed in the second half of 2007. Calculations were conducted at Mach of 0.8 and 0.85 with angles-of-attack of 0° and +3° for the tail-on configuration of one business jet model. The Reynolds number was 4.5 million as for the test.

Results

Figure 3 shows the results of the experimental and computational work. The near-field, far-field and total support effects are shown from left to right, and the contribution to drag, lift and pitching moment from top to bottom. The contribution of the total support is the combination of the near- and far-field effects. The results are shown for zero angle of attack only.

From the figure it appears that the far-field contribution to drag is partly compensated by the near-field effect of the Z-sting. For the total support, a Mach dependent correction is obtained, which is of the order of 20 drag counts up to Mach 0.7, increasing to about 35 counts at Mach 0.85. The far-field result was compared with the standard buoyancy correc-

German-Dutch Wind Tunnels

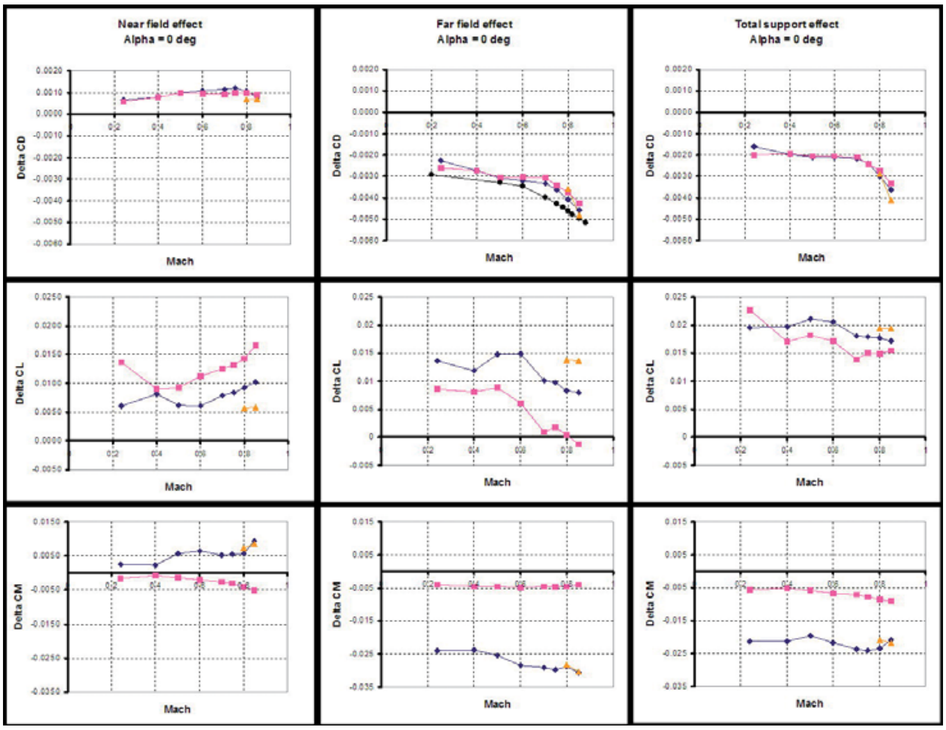

Figure 3: Experimental (exp) and computational (CFD) near-field, far-field and total support corrections for drag, lift and pitching moment. The model data are with tail-on and tail-off at zero angle-of-attack. Buoyancy corrections are shown for comparison with far-field corrections to drag.

tion of the common approach. It appears that the buoyancy correction over-predicts the experimental drag correction by about 5 to 9 drag counts depending on Mach number. This is attributed to the one-dimensional approach of the model cross-section used in the buoyancy calculations.

For lift, the contributions of near- and far-field effects are of the same order of magnitude. For the pitching moment, the far-field effects are even larger than the near-field contribution. This demonstrates the shortcomings of the common approach, and shows that the far-field effects need not only be taken into account on drag, but also on lift and pitching moment.

As stated earlier, there is a significant difference in lift and pitching moment for a model with and without its tail. Hence, it is important to include these configurations in a support interference test program. In addition to that, the support interference corrections show a dependency on angle-of-attack (not presented here) and Mach number.
It became clear that direct measurement of the total support interference not only gives better results, but can also be performed in about 30% less time, with respect to the common approach. In order to measure the total support interference, a configuration with and without dummy support was measured. The first configuration was measured using pitch and pause procedures, and the second in sweeps. Although the complete dummy support should have been removed from the test section, the time loss was less than measuring two runs with pitch and pause in the common approach.

CFD results are shown in Figure 3 for the infinite flow calculations at zero angle-of-attack. It appears that the agreement with the experimental data is rather promising. Differences are within five counts for drag, three counts for lift and two counts for the pitching moment. At higher angles-of-attack the agreement between computational and experimental data is however worse. This seems to be originating from incipient separation on the model, which results in less accurate CFD results. The infinite flow calculations produce similar results as the tunnel flow calculations, which are far more complex and time consuming than the infinite flow computations. Hence, the infinite flow approach seems to be the best approach for this kind of CFD analysis.

The CFD approach proved to be a valuable tool for validation of the experimental approach, as well as the investigation of detailed flow phenomena around the model and support system. As an example, the flow calculations showed that the design of the dorsal sting might be improved in order to reduce the wake behind the sting. At this moment, CFD cannot be used as an alternative for a complete support interference experiment. Further developments in CFD are necessary to perhaps replace the experiments in the future.

Conclusion

The investigation has resulted in an updated support interference procedure, with improved quality and about 30% reduction in time and cost with respect to the common approach.

Highlights of Project Work

Military Aircraft

External Store Testing with the Alenia Aermacchi M-346 D2 Model in the DNW-HST

Introduction

Military trainer aircraft are used to develop piloting, navigational or weapon-handling skills in flight. Typically, most contemporary military pilots after learning initial flying skills in light aircraft and ground-based simulators progress to a turboprop trainer. If they qualify for "fast jet" flying, they accordingly progress to a jet trainer. These jet trainers are capable of attaining high subsonic speeds and performing high-agility maneuvers, and are equipped with systems that simulate modern weapons, communication and surveillance technology for more advanced training. Most military training aircraft are twin-seat versions of combat aircraft types (ground-attack or interceptor) and can be converted in times of an emergency into a reconnaissance or combat aircraft (dual-use technology).

Alenia Aermacchi is a leading company in the design and production of trainer aircraft for military pilots. The newest generation of dedicated advanced/lead-in fighter trainers produced by Aermacchi is represented by the M-346. The aircraft is designed to the latest "design-to-cost" and "design-to-maintain" concepts with avionics modeled on those of the Eurofighter (Typhoon II), F-35 Lightning II, Rafale and other 5th generation combat aircraft. The M-346 exploits non-conventional features and advanced technologies. Vortex lift aerodynamics together with a full authority fly-by-wire flight control system allows it to remain fully controllable at angles of attack up to 40°. The maiden flight of the M-346 took place on 15 July 2004, marking the beginning of a comprehensive test campaign, involving upwards of 700 flights with three fully-instrumented aircraft for full flight envelope assessment and type certification.

High-speed tests in the HST

The tests in the HST 2.0 m x 1.8 m test section were the fourth in a series of consecutive tests that were performed with a 1:10 scale full-span model D2 of the M-346/S6, which was fully representative of the first two flying aircraft. The model was provided with two through-flow ducts for air intake simulation and an airbrake. The D2 model was heavily instrumented and had, beside an internal six-component balance of 2″ diameter, several secondary balances to measure loads on parts like the rear fuselage, wings, horizontal and vertical tail-planes and the nose droops. The horizontal tailplane was remotely controllable to save tunnel occupancy time. Extra added strain gauges enabled the measurement of loads on flaps, ailerons and rudder, while potentiometers recorded the position of the horizontal tailplane and rudder. Moreover, unsteady fin pressures were acquired by means of 16 additional Kulite sensors, eight on each side of the fin.

The model was mounted on the articulated boom support with a 5° preset short cone adapter. This adapter was provided with damping rings to reduce model vibrations, initiated by local flow phenomena. The setup allowed continuous variation of angle-of-attack over a range from -6° to +37° for sideslip angles of 0°, +5° and +10°, respectively. For store testing the model was equipped with external stores in two different configurations, fitted below the wings and the fuselage (see Figures 1 and 2). The store tests were carried out over a Mach number range from 0.2 up to 0.85 for all configurations (cruise, maneuver, take-off and landing) with the addition of control surface deflections. A series of high-speed tests in the cruise configuration were executed up to Mach 1.04 for buffet analysis. All low-speed tests were executed at the highest attainable pressure of 390 kPa, resulting in a Reynolds number of 16 million, while for higher Mach numbers the pressure was adjusted accordingly to maintain the highest possible Reynolds number.

Figure 1: Test setup with the 1:10 scale M-346 model mounted on the articulated boom support in the HST

Figure 2: Three-quarter rear view of the M-346 model with external stores, mounted in the HST

Test objectives

The test program included polars with all the main model control surface deflection configurations to determine overall model loads, part loads and control surface loads, including the recording of rms signals for unsteady loads analyses. Each test phase was preceded by a "back to back" measurement to verify the repeatability with past measurements for similar configurations. In addition, due to the intended similarity with both flying prototypes, the model is highly suitable for "back to flight" proof of testing, including unsteady load verifications on the tail-planes and rear fuselage. In this respect, the model represents a valued asset for verification of future configuration changes and system integrations.

A substantial part of the measurements was dedicated to buffet analyses. Wing buffet in the transonic flow regime is a result of shock-induced boundary-layer separation. The interaction can either cause boundary-layer separation beneath the shock leading to a separation bubble, or result in an early rear separation due to the increased susceptibility of the aft-shock boundary layer in an adverse pressure gradient. Both types of flow separation cause fluctuations in aerodynamic forces, which stimulate the aircraft structure, and thus lead to limitations in the flight envelope of the aircraft. The buffet boundary at a particular Mach number is the boundary in lift (or angle-of-attack) at which the flow is essentially attached and where the flow is totally separated and dominated by shock oscillations and large pressure fluctuations.

The buffet behavior of the Aermacchi model D2 was quantified with two methods. In both methods, wing tip accelerations deduced from measured wing root bending moment strain gauge bridge signals in the first bending mode were used as a measure of the response of the model to buffet excitation. For the analyses, the signals of the left-hand and right-hand wing root strain gauges and the right-hand flap strain gauge were acquired at a sampling rate of 1,024 Hz for approximately 200 seconds at various Mach numbers (typically 0.6, 0.8 and 0.85) for two steady angles-of-attack at buffet onset and with moderate buffeting. After conditioning and filtering, these signals were measured by the standard HST data acquisition system. The filter settings were verified by an LMS Fourier monitor. An example of unsteady loads and buffet onset and moderate buffeting conditions for a clean configuration are presented on Figures 3 and 4 for two different Mach numbers. Similar analyses were made for various store configurations. The combined results may be used to establish buffet onset envelopes for the pilots, while the buffet excitation parameters may be used for structural design analyses.

Conclusions

The tests for Aermacchi are a clear demonstration of the versatility of the HST to create a high-quality database, matching the requirements of modern military aircraft development.

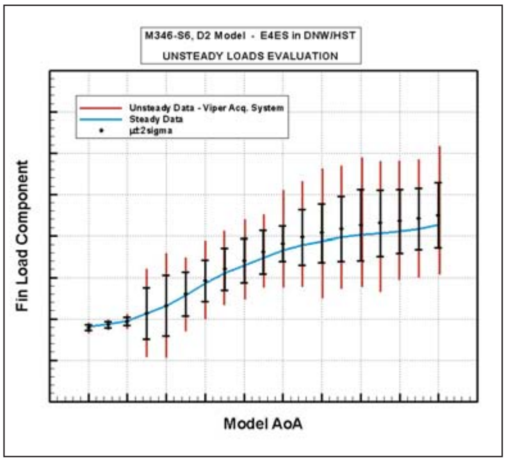

Figure 3: Typical example of steady and unsteady loads on the vertical tail of the D2 model of the M-346

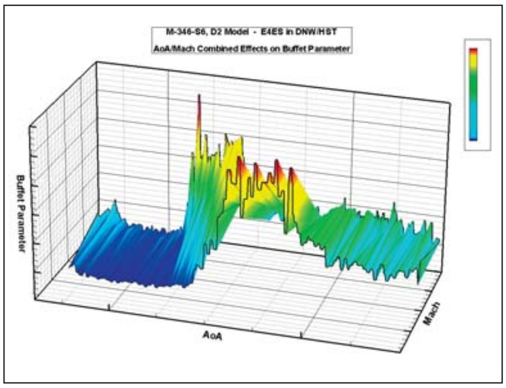

Figure 4: Typical example of buffet onset and moderate buffeting for a clean model at varying Mach number

Highlights of Project Work

Missiles

Testing of the IRIS-T SL Missile Model for Diehl BGT Defence

Introduction

The expertise of the DNW-TWG in testing different missile configurations has been described in some depth in our Annual Report of 2005, when Diehl BGT Defence (DBD) launched its first major development order with DNW. The reasons for testing in the TWG, as well as the compromises between the tunnel size, pressure levels and the flexibility and access were described in this report.

Since the TWG was not available for the follow-on testing planned by DBD for its IRIS-T SL missile in 2007, DBD decided to take advantage of the availability of the larger test section in the HST for the project. As far as the Mach-Reynolds number range is concerned, the more costly HST does not quite cover the required high Mach numbers, but can provide higher Reynolds numbers even at the same model scale. Furthermore, the Mach number capability of the HST can be complemented by our blow-down tunnel SST, which is operated as an additional test leg of the HST circuit.

Project overview and test objectives

The IRIS-T SL (Surface Launched) system is based on the concept of the IRIS-T air-to-air missile and complies with the German Air Force's new requirements for a secondary missile for ground-based, medium-range air defense within the trilateral MEADS program. Such requirements concern, for instance, high efficiency against a wide range of targets, high agility, short reaction time through vertical launch, target data synchronization via radio data link and easy logistics through storage, transportation and firing of the missile in the launch canister. Compared to IRIS-T, IRIS-T SL is equipped with a larger solid-propellant rocket motor, a data link and a nose cone for drag reduction. Via standardized "plug & fight" data interface, the IRIS-T SL system can be integrated into existing and future networked air defense command and controls systems. Compact carrier vehicles provide high off-road mobility and easy air transport in the A400M Airbus. IRIS-T SL is being developed within the TLVS/MEADS program and is planned to be in service from 2012.

During the initial phases of the IRIS-T SL development, a considerable number of configuration variants were analyzed, in order to optimize the aerodynamic configuration. For this purpose, a reliable database was required, which covered the whole operational flight envelope and beyond. This could only be obtained by experimental simulation in a wind tunnel.

High angle-of-attack tests in the HST

The tests in the HST were carried out with a 1:4.74 scale model (see Figure 1), which was essentially the same model as previously tested in the TWG. The model consisted of four replaceable parts (nose, transition cone with strakes and wings and an aft section with fins) and was equipped with aerodynamic control fins that were manually set to simulate roll, pitch and yaw configurations. The tests were executed in the HST 2.0 m 1.8 m test section with the model supported by means of a crank sting connected to a straight support boom (see Figure 2). Three crank stings were transferred from the TWG. A special adapter joined the crank sting to the boom roll adapter of the HST, which was provided by DNW. During the tests, three different stings were used with crank angles of 15°, 25° and 45°, which made it possible to extend the maximum incidence angle of the model from 30° to 40° and 60°, respectively. The remotely controlled roll variation possibilities of the TWG crank sting were incorporated into this test setup.

The internal balance arrangement used was the same as already applied in the TWG, where the balance position inside the missile model was varied in such a way as to minimize the occurrence of large moments due to large center of pressure variations with angle-of-attack.

The test Mach number was continuously varied from subsonic through transonic up to Mach 1.2. For higher Mach numbers, the SST provided both the Mach as well as Reynolds number capability.

For flow visualization the standard HST schlieren visualization system was used.

Figure 1: View of the IRIS-T SL missile model mounted in the HST

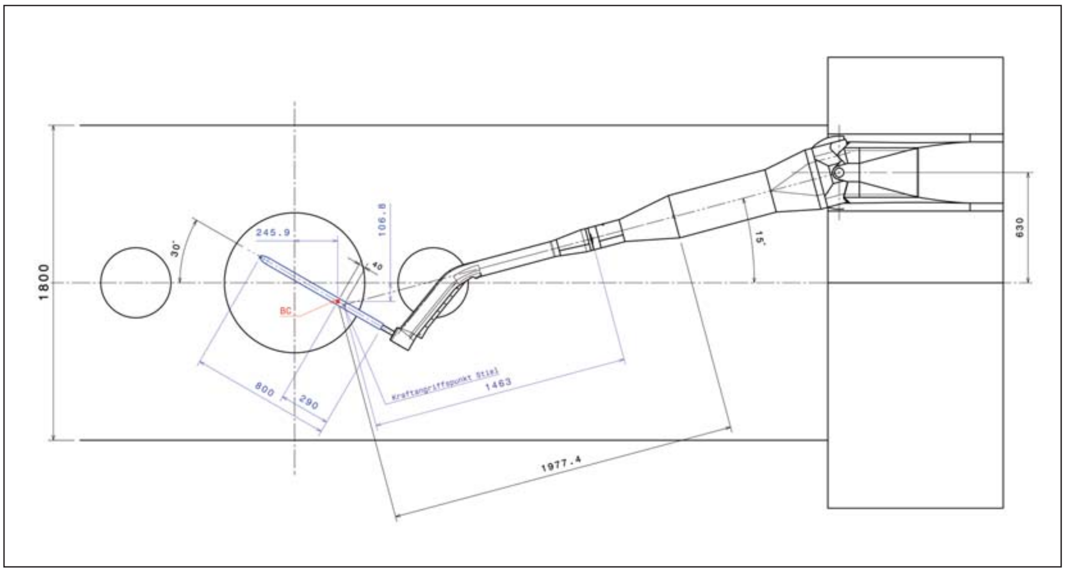

Figure 2: Schematic of the test setup with the 1:4.74 scale IRIS-T SL model mounted on a crank sting and the straight boom in the HST

German-Dutch Wind Tunnels

Results

One of the essential results of the test series in the HST was the demonstration of the reliability and compatibility of the aerodynamic simulations in the two transonic wind tunnels of DNW with the same model. The graph in Figure 3 shows that the aerodynamic coefficients obtained for an identical configuration in the TWG and the HST are in very good agreement. Figure 4 gives an impression about the large incidence range, which is covered by two remotely controlled crankings. Hence, it can be concluded that with respect to data quality for missile testing both wind tunnels, HST and TWG, deliver reliable results.

After the data quality had been proven, different wing and strake settings were tested to optimize the stability characteristics of the missile under crucial flight conditions. This analysis was strongly supported by DNW's sophisticated online data presentation system. A second part of the tests was devoted to the generation of a database necessary for six-degrees-of-freedom simulation purposes, control law design and evaluation of the flight performance of the missile.

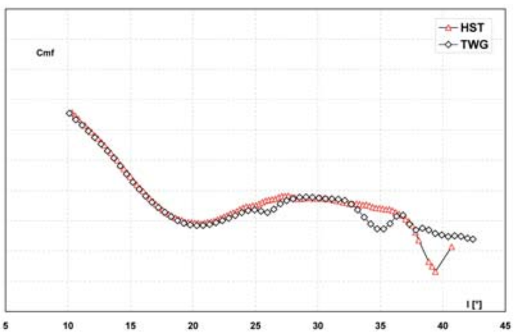

Figure 3: Comparison of pitching moment coefficients measured in the HST and TWG as a function of model angle-of-attack at one Mach number

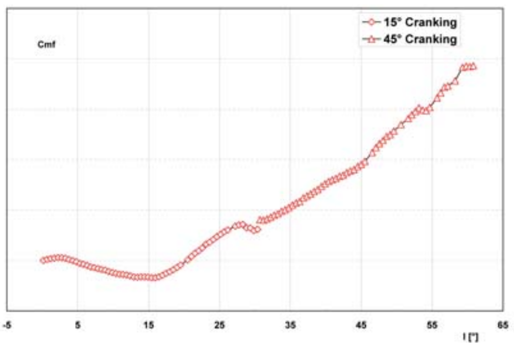

Figure 4: Graph of two incidence polars spanning the full angle-of-attack range up to 60°, obtained by using 15° and 45° crank stings at one Mach number

Conclusions

By combining the test hardware and test technique, already proven in the TWG, with the test hardware and test technique of the HST, it was possible to combine previous results with data from another tunnel in a short time. Since results from both tunnels were found to match, the confidence in the appropriateness of the test methodologies was confirmed.

The tests were an unprecedented demonstration of the value of redundancy in DNW's overall test capabilities. In this instance, an unscheduled interruption of testing in the TWG where this test was originally planned, was overcome by shifting the test to the HST, which minimized any delay for the Diehl BGT Defence.

Photographs released by courtesy of Diehl BGT Defence

Highlights of project work

Helicopters

Tilt-rotor Testing in the DNW-LLF

Introduction

Research into tilt-rotor technology began back in the 1940's with the Bell XV-3. The advantage of a tilt-rotor aircraft over a helicopter is the result of the latter's limitation in forward speed due to the lift loss on the rearward moving rotor blades. With the tilt-rotor, this problem is completely avoided because the propeller rotors are almost perpendicular to the motion of the aircraft in forward flight. Despite this advantage, the development of tilt-rotor aircraft knows a long history of ups and downs due to the complexity of the integration of the propulsion systems with the aircraft structure and the related handling and control aspects of flight physics and performance. Nonetheless, in the United States, with the support of NASA and the US Army, development efforts after several attempts resulted in a new tilt-rotor research plane, the Bell XV-15 in 1972. This effort subsequently led to the emergence of the Bell-Boeing V-22 Osprey twin-turboshaft military tilt-rotor craft, operational today. Meanwhile Bell, teamed with Agusta in Europe, started the development of the commercial BA609 tilt-rotor aircraft.

In Europe, tilt-rotor aircraft studies also know a long history, starting with compound helicopters and helicopters with stowed rotors in the early sixties. About twenty years later, joint studies were started between Italian, French and German companies resulting in the EUROFAR project for a 30 passenger, 14 ton commuter. Although this project could not be successfully concluded, two follow-up studies named EUROTILT and ERICA, were launched by Eurocopter and Agusta, respectively, in 2001. Both projects were supported by the European Commission. Since 2003, both Eurocopter and Agusta-Westland are taking part in a series of Critical Technology Programs (CTPs) of the

German-Dutch Wind Tunnels

European Commission as part of the European 5th Framework program to support technology research for future European civil rotorcraft. Two of these CTPs have participating partners in addition to the previously mentioned companies of system suppliers, research laboratories (CIRA, DLR, NLR, ONERA) and universities. These CTPs are concerned with rotor dynamics and acoustics (ADYN) and flight performance aerodynamics (TILTAERO). In the framework of these CTPs, two tests were conducted in the LLF, an aeroacoustic test in the three-quarter open-jet test section, coordinated and directed by Agusta in 2006, and a whirl flutter test in the 6 m x 6 m closed test section, coordinated and directed by Eurocopter Germany in 2007.

Figure 1: Schematic grid representation of the tilt-rotor model with dorsal sting support, for whirl-flutter analyses

Figure 2: Side-view of the LLF three-quarter open-jet test section with the tilt-rotor model on the external balance in hover mode

Figure 3: Downstream view of the LLF three-quarter open-jet test section with the tilt-rotor model in forward-flight mode, and acoustic instrumentation in place

Aeroacoustic test in the three-quarter open-jet test section

The model for this test was a 1:2.5 Mach-scaled half-wing replica of the ERICA concept, a tilt-rotor demonstrator equipped with a tilt-rotor nacelle and a tiltable outer wing part (see Figure 1). The model was tested in the three-quarter open-jet test section and mounted vertically on the six-component external balance of the LLF, below the test section floor, which was also the model's plane of symmetry (see Figure 2). The open-jet test section measures 6 m (height) x 8 m (width) x 19 m (length) and has a maximum velocity of 80 m/s. The floor used for these tests has a scoop system to remove the oncoming boundary layer air from the contraction. By rotation of the external balance, angle-of-attack variations were possible over a range from -180° to +180°. Two types of acoustic measurements were made. An out-of-flow acoustic array (4 m x 4 m), equipped with 144 microphones was used for noise source localization and relative strength determination by NLR. In addition, an in-flow microphone rake provided with 14 Brüel & Kjaer 0.5 inch microphones (with nose cones) was used for the determination and directivity mapping of absolute noise levels. Both, array and rake were mounted vertically at the starboard side of the tunnel (fly-over position for descent studies) on a floor-mounted traverse system, covering the length of the open-jet (see Figure 3).

The model rotor measured 1.85 m in diameter and was connected to the drive in the nacelle via a rotating balance. The wing span amounted to 3.5 m. The half-model consisted of three parts: the rotor-nacelle, the tiltable outer wing and the fixed inner wing. By means of a swiveling shaft, the rotor nacelle was connected to a platform underneath the floor for tilting the nacelle. This shaft ran into a second swiveling shaft that allowed both rotor and outer wing, to be tilted independently of one another. The loads on both wings were measured by strain-gauge balances. The overall loads were measured by the external balance. The rotor blades were the result of a common design effort by Agusta-Westland, Eurocopter, DLR and ONERA. Two out of four blades were instrumented with Kulite sensors and constructed and manufactured by NLR. The rotor was fitted with an electrical DC drive with a power output of 50 kW.

The major objective of the test program was to obtain insight in the noise characteristics of the rotor-wing model under the influence of rotor downwash and wake for different transient flight conditions, varying from hover via transition to forward flight and in particular for descent dominated by blade-vortex interaction noise. Typically, data sampling was chosen for a speed range between 0 and 55 m/s with the majority of the data at 40 m/s for different hub collective and cyclic pitch modes and wing tilt configurations. As rotorcraft, like helicopters, may operate at extreme flight conditions such as reverse flight or hover, a number of tests were carried out with the rotor at extreme angles with respect to the oncoming tunnel flow. To this end, the model was rotated by the external balance between +100º and -20º to match the setpoints of the test program. The advantage of the chosen setup was that it allowed for extensive database mapping at equal rotor thrust coefficients by on-line processing of the external balance. This setup enabled configuration variations to be made for trading off noise versus aerodynamics. Unfortunately, the tests had to be interrupted ahead of time, due to a shaft failure. They will be resumed.

Whirl flutter testing in the 6 m x 6 m closed test section

Tilt-rotor whirl flutter is an aeroelastic instability phenomenon, involving the propeller rotor, pylon, and wing. Historically, whirl flutter instabilities have been a matter of concern for propeller driven aircraft, since the loss of two Lockheed Electra aircraft in 1959 and 1960. Flutter is a dangerous phenomenon, encountered in flexible structures subjected to aerodynamic forces and is noticeable as a combination of bending and torsion motions. Flutter may be initiated by a small pitch-up rotation of the wing. As the increased lift force causes the wing to rise, the torsional stiffness of the structure tends to reduce the rotation, while the bending stiffness tries to return the wing to its neutral position. This may be followed by a pitch-down rotation of the structure and so on. As the aircraft flies at increasing speed, the frequencies of these modes coalesce to create one mode addressed as flutter resonance. The corresponding speed is known as the flutter speed. If the structural damping is insufficient, the oscillation amplitudes may diverge rapidly and can lead to dramatic consequences.

Flutter may be initiated by a number of phenomena such as fully separated flow (stall flutter), partially separated flow behind shocks (limit cycle oscillations) or engine whirl (whirl flutter). The latter involves a complex interaction of engine mount stiffness, gyroscopic precession forces of the engine propeller combination, and the natural flutter frequency of the wing. Whirl flutter is strongly dependent on the nacelle pivot location, stiffness and damping. As a consequence, wind tunnel tests to determine the whirl flutter speed limit require carefully scaled aeromechanical models of the wing, nacelle and propellers. For tilt-rotor models, this requirement necessitates that not only the structural masses and stiffnesses are properly simulated but also the relatively large propeller blades.

For the ADYN whirl flutter test, new aeromechanically scaled blades were designed by the ADYN consortium and produced by NLR as a follow-up to the initially designed blades for the TILTAERO program. The objective of the test was to explore the damping effect of the gyroscopic motion of the rotor on the whirl flutter behavior limits of the wing-rotor combination for speeds up to Mach 0.4. For this reason, the tests were carried out in the 6 m x 6 m closed test section of the LLF with the rotor freely wind-milling (see Figure 4). Contrary to the open-jet tests, the model was this time fixed to the multi-purpose turntable, which can be operated independently of the external balance. Prior to the wind tunnel test, ground vibration tests were performed by the DLR Institute of Aeroelasticity in the experiment hall of the LLF to determine the natural frequencies of the wing in bending and torsion. DLR was also responsible for analysis of the data during and after the test.

Figure 4: Tilt-rotor test setup for the ADYN whirl flutter tests in the LLF 6 m x 6 m closed test section

German-Dutch Wind Tunnels

The maximum attained speed during the tests was 138 m/s. The half-wing model was supplied by Agusta-Westland and fitted with two internal shakers in the nacelle to initiate excitation modes at a set speed for a particular model configuration (see Figure 5). The excitation system was provided and controlled by ONERA. Each shaker consisted of an electric motor to which an unbalanced mass was attached. The motors could either be rotated in phase with the masses set at 180° to simulate torsion excitation, or in counter rotation with the masses set at 0° to simulate beamwise excitation. The maximum flapping excitation was 6 Hz and the maximum torsion excitation was 12 Hz. An illustration of the test results is shown on Figure 6.

Conclusions

The complementary application of both open-jet and closed 6 m x 6 m test section, and the combined expertise of the consortium members and test crews are a clear illustration that extremely complex tilt-rotor tests can be handled fruitfully by a multidisciplinary international consortium.

Photographs released by courtesy of Agusta-Westland and Eurocopter.

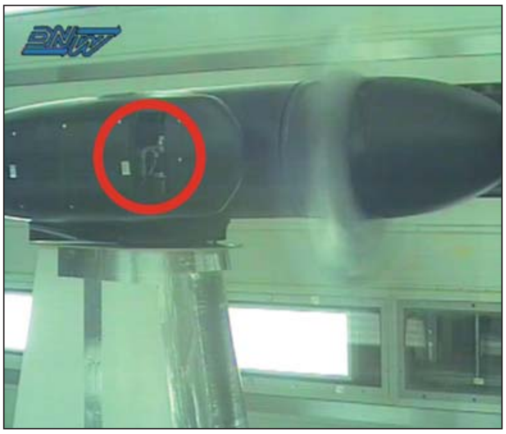

Figure 5: The tilt-rotor model's rotor-nacelle pictured during an ADYN whirl flutter test run with internal actuators (encircled) attached to the support structure

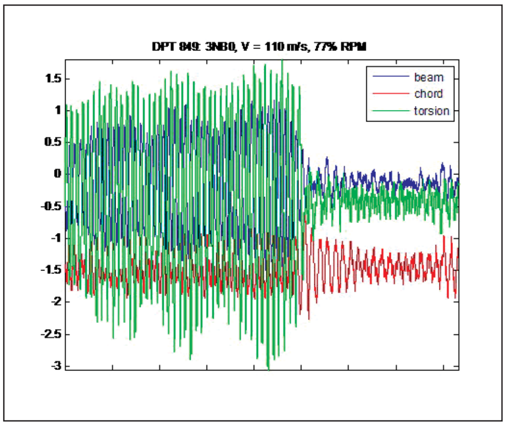

Figure 6: Typical signals from three strain-gauges mounted inside the tilt-rotor model during ADYN whirl flutter tests

Highlights of project work

Ground Vehicles

Passenger Trains in Wind Tunnels

Introduction

Although the increasing speed of the trains along tracks reduces the relative strength of the cross-wind component, its absolute value is of increasing significance to the stability of modern high-speed trains. This is partially true due to the weight reductions of the rolling stock, achieved in the pursuit of fuel efficiency and also due to the sensitivity of the streamlined configurations to aerodynamic effects.

In Europe, this topic has gained special attention and national guidelines for the assessment of cross-wind limits are available today. In the course of European standardization of regulations, the European Commission imposed that the cross-wind issue will be included in the High Speed TSI (Technical Specifications of Interoperability). This in turn requires agreement on a common European method for the determination of (a) the aerodynamic coefficients (drag, lift, side-force, and moments are very important for assessing vehicle stability), (b) the modeling of wind gusts and (c) the wheel-rail interaction forces (multi-body simulation). For this reason cross-wind stability is a key topic for the homologation of railway vehicles.

As will be discussed below, DNW has the capability to produce realistic and relevant simulations of the train aerodynamics, both for the fundamental understanding of the effects as well as for quantitative evaluation of various track situations. Here rolling stock in the flat plain, high embankment and tracks on bridge configurations are all considered.

Experiments

Since one of the most important phenomena in the cross-wind situation is the flow separation above the roof of the train, with the separation pattern

German-Dutch Wind Tunnels

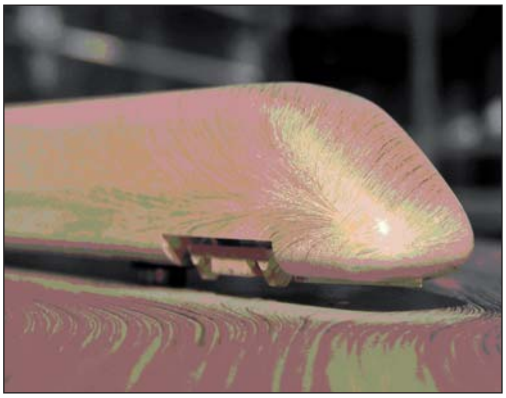

Figure 1: Surface oil flows on the ICE 2 model end car, with a yaw angle of 40° and flow speed U∞ = 30 m/s, (Re = 2.25 million) in open plain configuration.

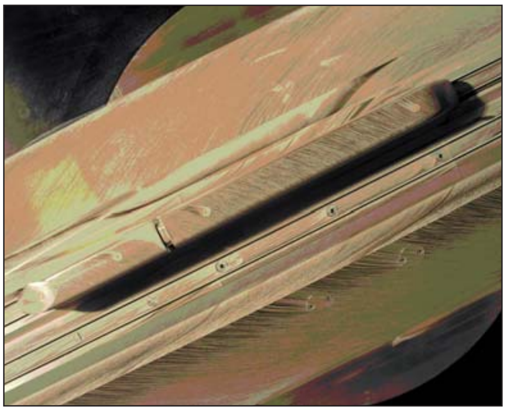

Figure 2: Surface oil flows on the ICE 2 model end car, with a yaw angle 30° and flow speed U∞ = 30 m/s in a high embankment configuration with the train on the leeward track in accordance with TSI provisions

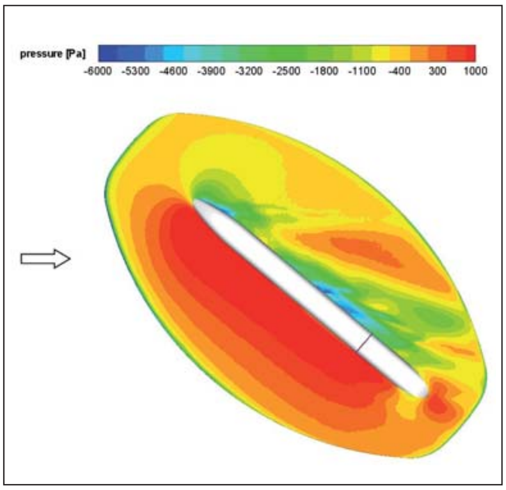

Figure 3: DLR RANS computed pressure distribution around a train sitting on the splitter plate in a cross-wind condition and open plain configuration

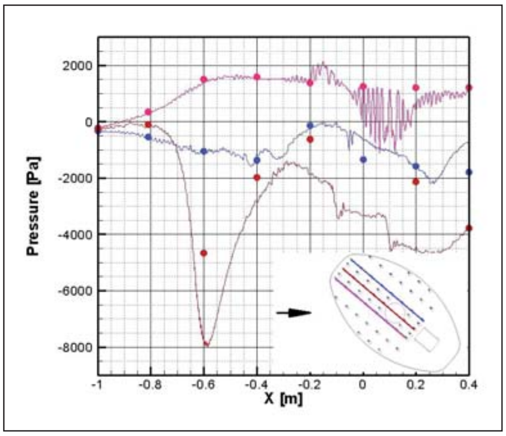

Figure 4: Comparison of experimental (dots) and numerical pressures (lines) along different pressure tap rows on the splitter plate for a cross-wind condition and open plain configuration

expected to depend not only on the geometrical boundary conditions, but on the Reynolds number as well. Therefore, testing in conditions of high and independently variable Reynolds numbers is of paramount importance, to obtaining reliable information. For this task, two of the wind tunnels operated by DNW are perfectly suited: the DNW-HDG and the DNW-KKK. In the HDG, the required high Reynolds number is achieved by pressurizing the whole wind tunnel. Maximum pressure obtainable is 10 MPa (100 bar); characteristically the tests take place at 6 MPa. In the KKK, high Reynolds numbers are achieved at atmospheric pressure by lowering the ambient temperature through addition and evaporation of Liquid Nitrogen (LN_2) into the wind tunnel circuit.

The models used in the HDG and the KKK were built at 1:100 and 1:25 scale of the modern trains ICE2 and Next Generation Train NGT, respectively. The Reynolds numbers tested here were up to 3 million for force measurements. In the HDG, even higher values are possible, although this capability was not used in the tests reported here.

Flow field studies

The patterns surface flow patterns around the train model were visualized by means of oil flow in the HDG. For flat ground visualization the 1:100 model was equipped with a dummy end car to provide a realistic wake simulation, and mounted on a splitter plate in order to remove the effects of the wind tunnel wall boundary layer. A series of yaw angles between -60° and +90° were tested, of which Figure 1 shows an example. For visualization of the surface flow pattern when the train was on a high embankment, only a yaw angle of 30° was used. Figure 2 displays the pattern where features characteristic for the embankment can be identified.

Surface oil flow visualization was not available in the KKK. However, the splitter plate on which the train model was mounted could be equipped with an array of 57 pressure sensors distributed over the complete surface. The results of these pressure measurements were interpreted with the help of numerical calculations performed with the DLR RANS code. The existence of a vortical structure in the flow field on the leeside of the train, suggested by the calculations (see Figure 3), is supported by the pressure measurement results compared with the calculations on Figure 4. However, the magnitude and strength of the measured and numerically simulated vortices differ, confirming the need for further research.

In addition to studying the surface flow patterns, the cross-wind induced separated flows were quantitatively measured by means of Particle Image

Velocimetry (PIV). PIV reference measurements were made in the DLR 1-meter low-speed wind tunnel; the PIV equipment consisted of two 12 bit cameras with a resolution of 1280 x 1076 pixels. In the KKK, the single camera used had a resolution of 4008 x 2672 pixels. In the case of the 1-meter tunnel a double-pulsed Nd:YAG laser with 50 mJ output was sufficient; in the KKK the output power was 320 mJ per pulse. On Figure 5, two characteristic results are presented. The differences between the flow with and without embankment are striking. In the presence of the embankment, the flow is already strongly accelerated, even before reaching the train itself, leading to streamline curvature in the approaching flow field. Additionally, there is a strong Reynolds number effect, although due to the technology requirements, the PIV result from KKK is shown at a low, non-cryogenic Reynolds number condition.

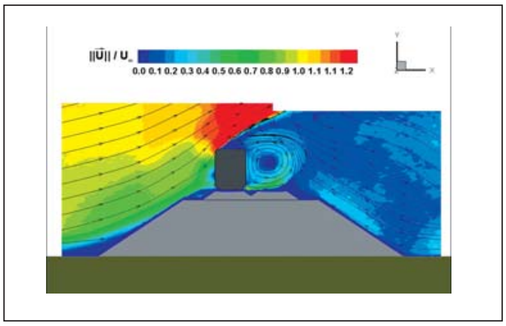

Figure 5a: Train model PIV velocity map and streamlines with a yaw angle of 90° and a flow speed U∞ = 30 m/s in a high embankment configuration (Note: these measurements were performed in the DNW 1 m wind tunnel in Göttingen)

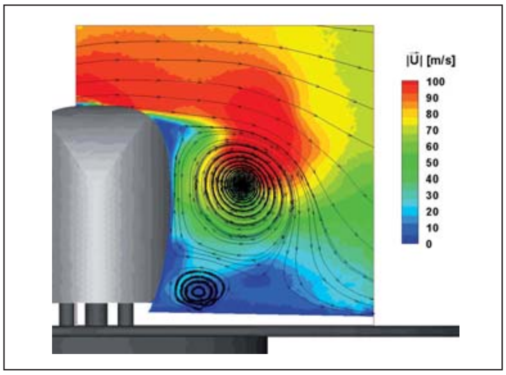

Figure 5b: Train model PIV velocity map and streamlines measured in the KKK with a yaw angle at 40° and flow speed U∞ = 90 m/s (Re = 0.73 million) in open plain configuration

Side forces

In the test entries where the surface flow was studied, the models in both tunnels were mounted on external six-component balances in both HDG and KRG. Thus, it was also possible to obtain quantitative data about the side-forces and rolling moments acting on the respective models, relevant for the evaluation of stability of the rolling stock. Both, averaged as well as instantaneous information can be presented. It is significant, that the instantaneous values of e.g. the side-forces can be of up to 30% higher than the average values and need to be properly accounted for in the evaluation of the vehicle stability (see Figure 6). A correlation between the instantaneous load and the position of the leeside vortices may be suggested.

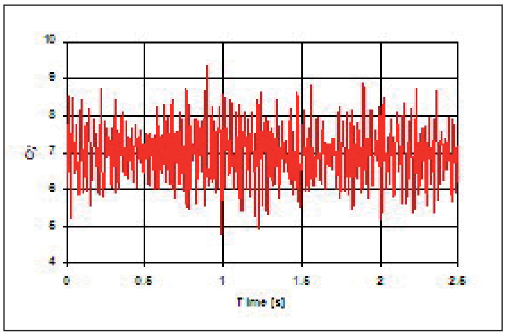

Figure 6: Unfiltered side-force signal for the train model in the KKK at a yaw angle of 40° with a flow speed U∞ = 90 m/s

Both, the side-force measurements in the KKK (see Figure 7) as well as the rolling moment measurements (see Figure 8) shown here for a result from the HDG, display a monotonous behavior up to negative and positive yawing angles of approximately 60°. Thereafter the magnitude of the respective effect starts to decrease again.

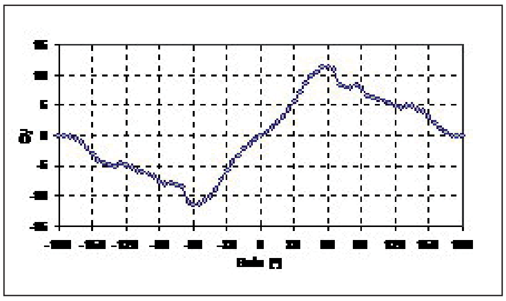

Figure 7: Graph of steady train side-force measurements taken in the KKK for a full 360° of yaw with flow speed U∞ = 90 m/s (Re = 0.73 million).

Outlook

Due to the requirements imposed by high-speed travel, the train tracks cross a large part of the terrain on long and high bridges, increasing the exposure of trains to strong cross-winds. The bridge corpus affects the flow field around the train through its own displacement effect. There is a need to establish a correlation between the stability of a train in flat ground configuration and on the bridge. Work on experimental simulation of the train-on-bridge configuration in the HDG has been started by DLR. The experimental setups are shown on Figure 9a and b and the analysis of the results is ongoing.

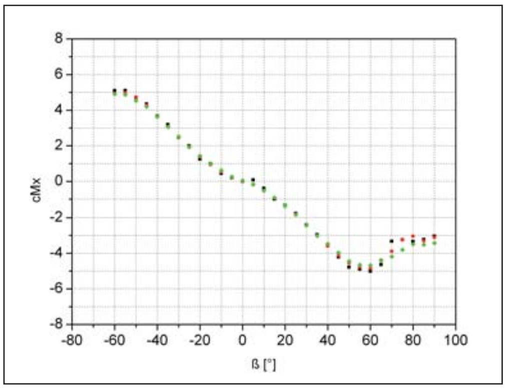

Figure 8: Graph of train rolling moment versus yaw angle, measured in the HDG

German-Dutch Wind Tunnels

Figure 9a: HDG test setup with a model of two ICE 3 end cars back-to-back in train-on-bridge configuration with a yaw angle of 90º

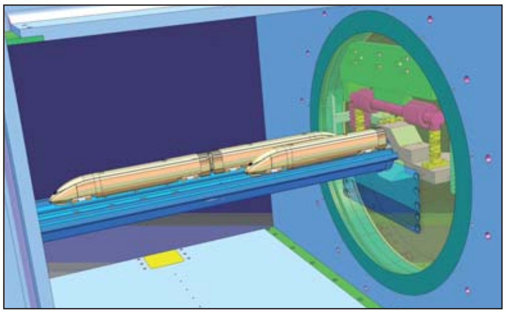

Figure 9b: Schematic of two possible model setups in the HDG, with either one or two ICE end cars in train-on-bridge configuration, with a yaw angle of 90º. Note: Only one configuration was used at a time

Due to the increased requirements for speed and reliability of train travel the world over, DNW expects to remain a steady and qualified supplier of wind tunnel reference data to the research, development and certification of high-speed trains.

With contributions from DLR-AS

Aeroacoustic Testing of MAN Trucks TGX and TGS

The MAN Group is one of Europe's foremost industrial players in the sector of transport-related engineering. The group's business units hold leading positions in their markets, which may be illustrated by the election of the MAN trucks TGX/TGS as Truck of the Year 2008. Part of this award may be attributed to aerodynamic and aeroacoustic research, resulting in reductions in drag and noise levels compared to previous designs.

Aerodynamic research of truck vehicles at MAN Nutzfahrzeuge possesses a long history of continuing efforts to improve the driving performance and the safety of road transport. At MAN at least, five types of investigations are distinguished. These are:

- Performance improvement by drag reduction of trucks and truck-trailer combinations
- Engine performance and sustainability improvements by efficient cooling of the motor
- Cabin climate improvement by enhanced cabin ventilation for the driver
- Window and mirror visibility augmentation by reduction of dirt contamination
- Cabin noise reductions to augment the comfort for the driver

Beside economic advantages, the first two applications are directly beneficial for the environment as they lead to less CO_2 and NO_x emissions. The latter three applications contribute each in their own way to less fatigue of the driver and thus to better road safety. Hence, economy, environment and safety are key drivers for aerodynamic research by MAN, with DNW support.

The aerodynamic development process at MAN is based on a threefold approach, starting with in-house Computational Fluid Dynamics (CFD) calculations, followed by verifications tests at 1:4 scale in the NWB and then full-scale validation tests in the LLF. The full-scale tests were required in order to improve details that were hard to realize at model scale and for final verification of the proposed configuration preceding serial production. This approach has also been applied to the development of the new TGX/TGS trucks by MAN. An essential part of these tests consisted of noise reduction by localization, followed by elimination or attenuation of the dominant noise sources.

Acoustic measurements

For the detection of noise sources, DNW applies so-called acoustic arrays, consisting of an arrangement of microphones, typically located on the walls of the test section. The identification of noise sources is based on the principle of beam forming, by use of the differences in path lengths between a particular source and the individual array microphones. As result of the difference in propagation time, each microphone receives a signal with different amplitude and phase. These differences are used to determine the location and the strength of the source after phase shifting and summation of the microphone signals for a particular frequency (see Figure 1). The size of the array system and the number of microphones depend on the frequency range of interest together with the size of the test object.

A typical result after processing of the acoustic array data is a source plot, which contains the locations and the differences in magnitude of the individual sources by color coding of the noise levels in 1/3 octave frequency bands (frequency domain) projected on the geometric shape of the test object. These source plots enable a rapid assessment of the dominant sources to be made, so that during a test campaign corrective measures can be initialized, to eliminate or reduce the noise contributions of a particular source.

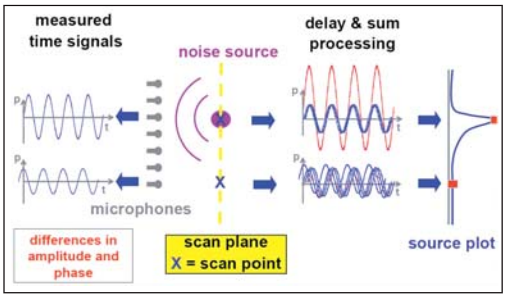

Figure 1: Schematic of the microphone array technique for the detection of noise sources

Testing in the NWB

In cooperation with MAN, the NWB developed a special floor for testing of 1:4 scale truck models. The TGX/TGS scale models were placed on a turntable and fixed with pins from the tyres via a solid pad-beam structure to a six-component external balance underneath the floor. The balance provided force and moment data for a set angle of yaw. The yawing range of the turntable was ± 10°. For acoustic testing, two wall arrays of 1 m^2 each carrying 144 microphones were placed on the top wall and starboard sidewall of the test section (see Figure 2). The tests are executed at speeds up to 80 m/s, to achieve Reynolds numbers corresponding to the full-scale truck at road travelling speed.

The acoustic arrays enabled a clear view of the noise sources on the roof and right-hand side of the truck model. DNW provided the on-line processing and presentation of the array data for verification and comparison with different model configurations. Additionally, off-line processing was provided as well, to support the on-line conclusions and enhance the accuracy of the on-line results. Figure 3 shows typical 1/3 octave band sound pressure level source plots for one configuration at four different center frequencies. The color code is a measure of the intensity of the noise levels over a 12 dB range.

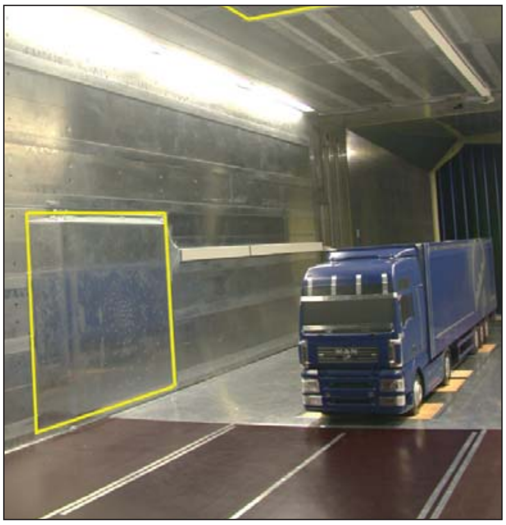

Figure 2: NWB test section with 1:4 scale TGX model truck and microphone wall arrays (outlined in yellow)

The results indicate that, depending on frequency, dominant noise sources are wing mirrors and front spoilers, while at the lower end of the frequency band the bumper and the cavity between truck and trailer are of significance.

The attractiveness of the wall array technique is clearly illustrated on Figure 4, which shows a comparison of two source plots with identical center frequency for two different wing mirror configurations. The combination of simultaneous acoustic measurements with the wall arrays and drag measurements by the external balance allows for rapid optimization of such configurations. It requires little imagination to realize the benefit of the combined techniques for selection of the best configuration at a quarter-scale, before proceeding to the more expensive verification tests at the LLF.

Testing in the LLF

The tests in the LLF were carried out as usual in the 9.5 m x 9.5 m test section. This section has a length of 20 m and can accommodate full-scale truck-trailer combinations. The truck-trailer combination floats by means of thin air cushions under the wheels on a special floor insert and is accordingly connected by a central strut to the under-floor external balance. The setup allows for three-component measurements in drag, side-force and yawing moment over a yaw angle range of ± 15°. The tests are typically carried out at speeds of 80 km/h, typically. Like in the NWB, microphone wall arrays enable simultaneous measurements of acoustic with force and moment data.

Although the source plots (see Figure 5) illustrate a striking similarity with the data of the NWB as expected, considerably more detail can be observed in the LLF data due to the presence of all small full-scale parts that are hard to realize at quarter-scale. Another advantage of these full-scale tests is that they enable the client to place a dummy driver in the truck cabin, which is fitted with ear microphones and recording equipment (see Figure 6). The noise at the dummy's ears is used to study the drive cab environment, and identify the internally dominant contributions of externally visible noise sources, as seen on the source plots. The combina-

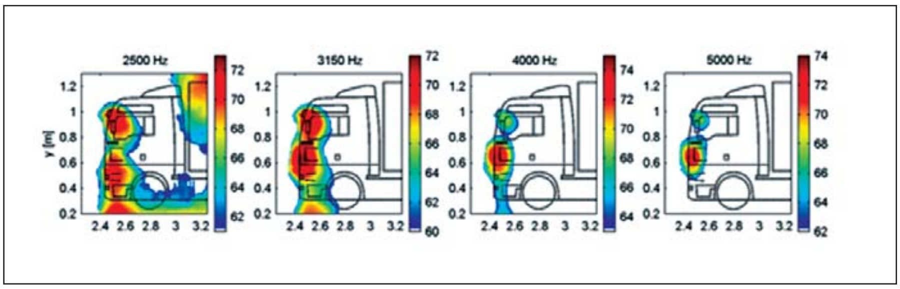

Figure 3: Source plots made from the microphone wall array measurements in the NWB, using four different center frequencies

tion of both measurement techniques (as in the NWB) allows a trade-off between measures to reduce noise from external sources and the impact on drag or dirt contamination. Among the sources studied in this respect were the mirrors, the bumpers and spoilers, the A and B columns, the roof, and the radiator.

Conclusion

The cooperation between MAN Nutzfahrzeuge and DNW has enabled the client to profit from the noise expertise of DNW. This expertise was gained by implementing novel acoustic techniques originally developed for aeronautical research and the aerospace industry. Moreover, the application of the NWB as pilot facility is a fine example of how tests in the more expensive LLF can be prepared optimally by conducting experiments at model scale, thus saving cost and time for the client.

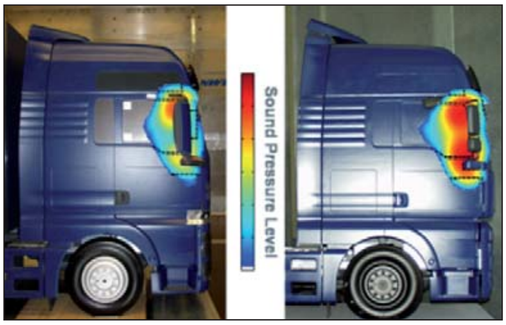

Figure 4: Comparison of sound pressure levels with identical projected center frequency plots for two wing mirror configurations

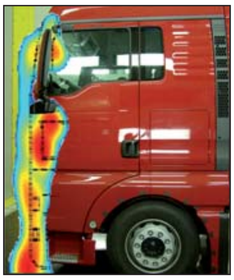

Figure 5: Projected source plot on the port side of a MAN truck-trailer combination in the 9.5 m x 9.5 m test section of the LLF

Figure 6: Dummy driver with ear microphones and data acquisition and processing equipment inside the truck cabin during LLF testing.

German-Dutch Wind Tunnels

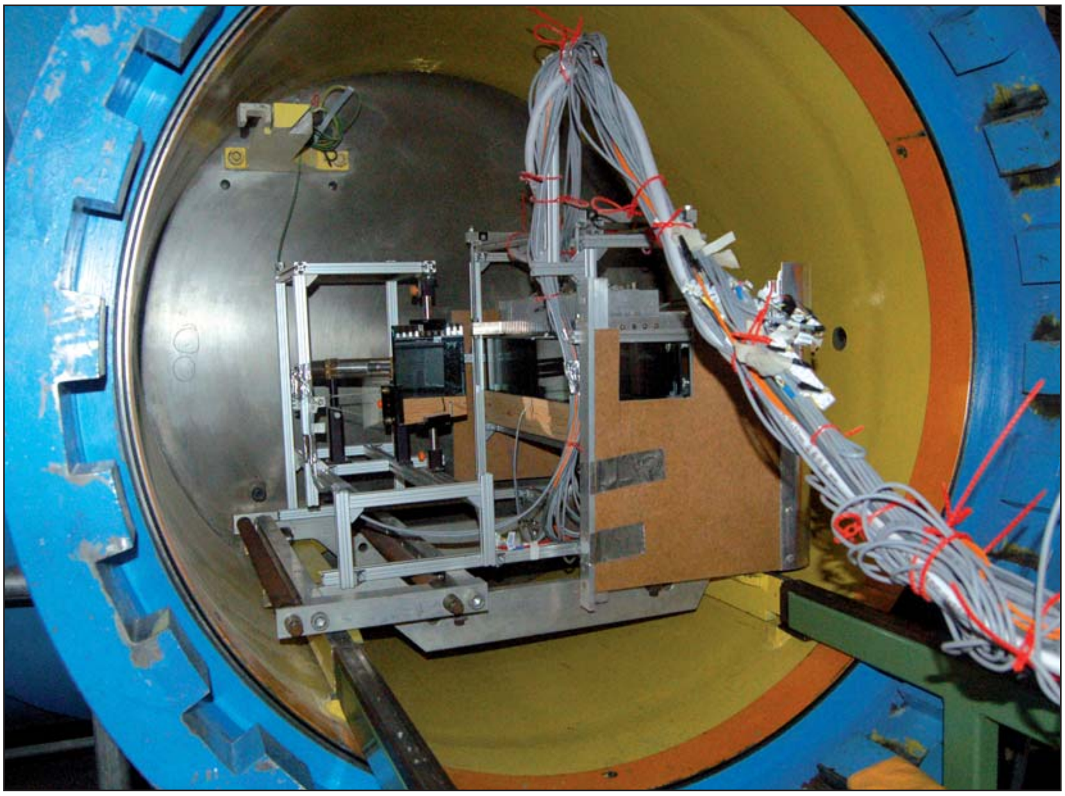

Highlights of Project Work

Environmental Engineering

Scaling of Turbulent Mixed Convection in the DNW-HDG

Introduction

Mixed convection is the superposition of forced and free convection. It occurs in many technical applications and configurations like heat exchangers, air conditioning of passenger compartments or climatization. Moreover, mixed convection is a typical phenomenon in geology and meteorology.
Measuring large-scale mixed convection at full-scale can be difficult, or even impossible. Hence, experimental acquisition of mixed convection at reduced model size, using aerodynamic scaling, is a promising approach, which allows large-scale flows to be investigated on a laboratory scale. Also motion, heat transfer and scaling of mixed convection for an enclosed fluid, heated from below and cooled from above, especially at high Grashof (Gr) and Reynolds (Re) numbers, still lack explanation of many fundamental phenomena.
To progress this research effort, a convection cell (see Figure 1), for testing in the high-pressure wind tunnel HDG, was developed to study mixed convection for $600 < Re < 3 \cdot 10^6$ and $5 \cdot 10^5 < Gr < 5 \cdot 10^{10}$, with air as the working fluid, using Particle Image Velocimetry (PIV). The convection cell consisted of a cuboidal container with a quadratic cross section, an air inlet at the top and an air outlet at the bottom (see Figure 2). The cell was 0.1 m wide, 0.1 m high and 0.5 m long. In- and outlet were both located on the same side of the cell. Both, the air in- and the outlet, spanned the whole length of the cell and consisted of rectangular channels, with a channel height of 5 mm and a length of 300 mm for the inlet, and a channel height of 3 mm and a length of 120 mm for the outlet. The inlet channel was equipped with an additional fence to further homogenize the inflow. All side-walls were thermally insulated by a layered system, which consisted of an insulating sheath of 7 mm air between two layers of transparent windows, to achieve almost

adiabatic boundary conditions while, maintaining the optical access to the cell.

In order to cover the ranges of Re and Gr, the convection cell was designed to be operated in the HDG over a pressure range of $1 < p < 100$ bar, and to be accessible to PIV. The function of the HDG in the experiments was threefold. Firstly, it allowed adjusting the fluid pressure, secondly, it provided the inflow to the convection cell, and finally it supplied cooling to the cell ceiling.

The main objective of these studies was to improve the understanding of flow and heat transport in mixed convection for high Re and Gr values. Of particular interest was the dependency of the flow structure and heat transfer on the ratio of buoyancy and inertia forces. Another important aim of the experiment was to develop and prove a scaling theory, which would allow scaling of the spatial dimension of mixed convection to an experimentally accessible size by increasing the fluid pressure and the inflow velocity.

Figure 1: Generic convection cell for mixed convection studies in the open lock of the HDG

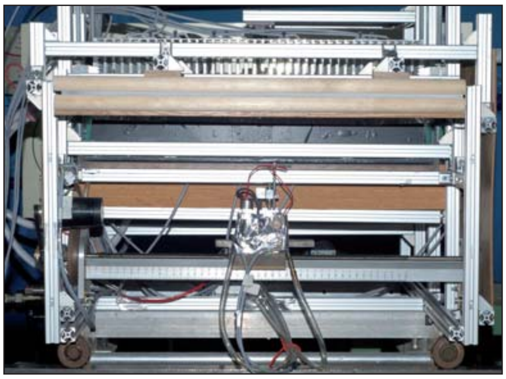

Figure 2: Front view of the convection cell in the HDG with the air inlet located at the top and the air outlet at the bottom

Measurement in the HDG

In April and May 2007, a first measurement campaign of mixed convection was performed at the HDG. The PIV measurement technique had already been successfully applied under the special conditions of the HDG. The main challenge consisted of the choice of the tracer particles and the limited optical access. Two kinds of solid tracer particles, Expancel, a polymer microspheres, and Matroxid (Al_2O_3) were tested. In conclusion, it turned out that Matroxid, with a mean diameter between 2 and 3 µm, provided the best results. The particles were injected into the flow by a fluidized-bed seeding generator (see Figure 3). The light sheet was coupled into the HDG by one of the front windows and the camera was attached to the other. In addition to PIV, temperature measurements were performed.

Figure 3: Fluidized-bed seeding generator

Figure 4 shows some results of the PIV measurements at $p = 5.1$ bar, $Re = 6.0 \times 10^3$, $Gr = 9.2 \times 10^7$ and thus the Archimedes number $Ar \approx 1.6$. The upper left plot reveals the time-averaged velocity fields (air in- and outlet are shown top and bottom on the right-hand side, respectively). The upper figure on the right-hand side depicts an instantaneous velocity field. The lower left-hand plot shows the coherent structure of the first mode of a Karhunen-Loewe procedure, which was a roll structure induced by the forced convection. The lower plot on the right-hand side shows the coherent structure of the second mode, which was induced by free convection. Particularly in this region of Ar, a superposition of a transversal (forced convection) and a longitudinal structure (free convection) was observed. A periodic recurring of these structures is found by analyzing the time-dependency of the 2D in-plane flow field.

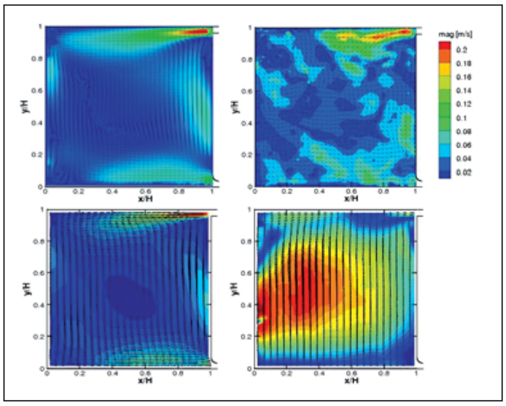

Figure 4: (a) Upper left: Time averaged velocity field, (b) Upper right: Instantaneous velocity field, (c) Lower left: First mode coherent structure, (d) Lower right: Second mode coherent structure

Figure 5: Spectrum of the outlet temperature time series (lower data set) and of first three mode's time series

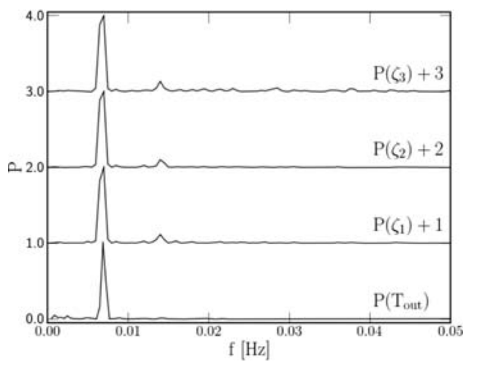

This oscillation can be observed in the power spectrum of the outlet temperature time series. This frequency can be found also as a characteristic frequency of the first three mode's time series (see Figure 5).

Conclusion

The pressure dependency of the dynamics of coherent structures mixed convection was investigated in a rectangular convection cell. This study was performed at stagnation pressures 1 and 15 bar using PIV and temperature measurements. The PIV measurement technique was adapted for application in the HDG. As a next step, it is planned to perform detailed temperature measurements, in an effort to obtain more information on the dependency of the heat transfer on the fluid pressure. Furthermore, in the longitudinal direction, stereo PIV measurements are planned.

Contributed by A. Westhoff (DLR)

Technical Status

The LLF is an atmospheric, closed circuit low-speed wind tunnel that has been in operation since August 1980. After more than 25 years, a number of original systems was due for replacement. The first aim of such renewals is to keep the wind tunnel operation reliable. Besides, upgrades present the opportunity to implement up-to-date equipment and techniques, and the operation and maintenance of systems may then become easier. If measurement systems are replaced, data quality improvement is often possible. In 2007, four large replacement projects took place, involving: the sting support fairing, the fan drive controls, the flow reference system, and the sting controls. The fan drive modernization required a tunnel downtime of about six weeks, in which also the flow reference system and the sting controls were replaced.

Replacement LLF Sting Support Fairing

The horizontal rear part of the LLF sting mechanism is named torpedo and its cover is called sting torpedo fairing. The purpose of this fairing is to guide the tunnel flow smoothly around the sting support mechanism. Besides, the fairing protects the equipment attached to the support mechanism, e.g. cabling, connectors, and hydraulics. The old fairing consisted of aluminum plates on an aluminum frame, fastened to the sting by bolts. The seams between the plates were taped (see Figure 1). Tests with fighter models with strong vortices in their wake caused abnormal wear of the construction. Frequently, bolts (several hundreds) became detached and were often carried away with the air flow with the risk of damaging the fan blades. Repairs led to delays in the test operation, and this alone would be enough reason for refurbishment. However, also oil leakage from hydraulic lines inside the fairing caused substantial

German-Dutch Wind Tunnels

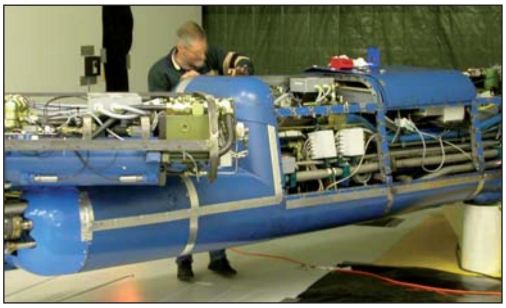

Figure 1: Old LLF sting support fairing with access panels removed

Figure 2: New LLF sting support fairing with the upper cover being removed

smearing of the tunnel circuit, and accessibility to the sting equipment was poor. Moreover, normal wear and visual aspects (e.g. dents, scratches, and cracks) were additional reasons to renew the fairing.

The new fairing had to fulfill the conflicting requirements from the aerodynamic and engineering points of view. For aerodynamic reasons, it was not possible to go beyond the outer dimensions of the old fairing. Therefore, it was only possible to maximize the interior space with the same outer dimensions. All other requirements came from engineering and operational considerations. The major requirements comprised:

- Strong, rigid construction without any underlying framework
- Easy access to the sting equipment and cabling
- Leak-free catchall to avoid oil smearing of the circuit
- Quick locks instead of bolts at the service hood
- Simple mounting of tubes at the lower side of the torpedo

The upper side of the fairing is made from carbon fiber with a honeycomb profile. The lower cover is made from solid glass fiber forming a leak-proof catchall.
The fairing parts were fabricated using molds. Firstly, a wooden plug was made with the outer dimensions of the sting fairing and this was then used to construct the mold itself.

The new fairing meets the requirements regarding rigidity and ease of access and is leak-free. Part of the upper cover can be easily removed (see Figure 2). Immediately after its installation, the fairing was proven to withstand the extreme conditions in the wake of a fighter model during a one-week tunnel entry.

LLF Fan Drive Modernization

The LLF is driven by a single-stage fan with eight non-adjustable blades of 12.35 m diameter. The fan is directly coupled to the shaft of the direct drive, variable speed synchronous electric motor (Siemens), completely enclosed in a nacelle, with a continuous maximum drive power of 12.65 MW at 225 rpm.
The maximum achievable speed in the different test section configurations of the LLF, characterized by their width x height in meters, is:

• 8 x 6	110 m/s
• 6 x 6	145 m/s
• 9.5 x 9.5	60 m/s
• 8 x 6 open jet	80 m/s

Although a complete replacement of the fan drive system including motor was considered, eventually it was decided to restrict the upgrade to the AC drive, the motor controls, and the related equipment. The limitation of scope was possible due to the refurbishment of the Siemens motor a few years ago and the lack of wear. But certainly as important was the avoidance of the much higher cost and the longer downtime of the wind tunnel involved, as the replacement of the motor would entail opening of the fan housing and shelter.

The main reasons for the replacement of the control system were the aging of the hardware, the lack of availability of spare parts, and the disappearance of the external know-how. Without renewal measures, maintenance problems would undoubtedly occur in the near future. The replacement had to result in higher reliability for the next decades.

The new system had to cover at least the existing control range, preferably with better control characteristics, and reach the same speed of control and accuracy as the old system. Besides, the performance of the motor was not allowed to deteriorate. There was a preference for a standard control system available off-the-shelf, requiring only normal maintenance during its lifetime.

After a thorough selection process, ABB was chosen out of three possible suppliers. During the selection, the state-of-the-art control technique and the extent of compliance with the requirements were the main factors. But also the possibility to provide a retrofit solution, i.e. the control system adapted to the existing drive motor and the availability of long-term maintenance support, were important aspects. A specially adapted transformer (see Figure 3) from the product line ABB Resibloc and a medium voltage drive ACS 6000, also a standard product, were selected. Such AC drives are used to control the speed and torque of synchronous machines, where high powers are needed. By providing precise process control, the drive ensures the highest control accuracy, despite input power variations or sudden load changes. This technology guarantees a constant flow velocity in the test section, and hence accurate wind tunnel measurements.

The new fan controls are located in a large container (180 m^3) next to the fan house. The container was placed on a cellar to make the power cables easily accessible during the installation of the system (see Figures 4 and 5). Owing to this container solution, the major part of the preparatory work could be performed without blocking the operation of the tunnel. The hardware could be pre-installed to a large extent in the container before delivery. As a consequence, the downtime of the wind tunnel was limited to six weeks.

The replacement of the fan controls was a technically complex project. Therefore, a phased approach was chosen with much attention paid to the different technical possibilities during the initial phase. The project started mid-2005 and the preparatory construction work on site started in the second quarter of 2007. The system was ready for operation in October 2007. Besides the supplier of the major system, a considerable number of other contractors were involved for construction work, cabling and the PLC system. The new system is prepared to communicate with a data management system in the future. There are several additional benefits owing to the renewal:

- The status of the drive motor is known
- The critical eigen frequency of 300 HZ of the drive motor, obviously generated by the old system, has disappeared
- The disturbances in the power grid have disappeared
- The new software tools and the option for remote service facilitate the maintenance of the system

Replacement LLF Sting Support Controls

The sting support system is the main model positioning system of the LLF, with a total mass of about 30 tons. An aircraft model equipped with an internal strain-gauge balance and on-board instrumentation can weigh up to 2 tons. The model support arm in its initial horizontal position has a length of about 10 m. Sting motions in pitch, yaw and the vertical direction are achieved by hydraulic power. The total pitch range is 60° (typically -15° to +45°). The total yaw range is also 60° (-30° to +30°). The required accuracies of set pointing under static conditions are 0.01° and 1 mm. The function of the sting support controls is to operate, monitor and safeguard the sting position and attitude and to perform the acquisition of position and attitude data.

Figure 3: Hoisting of the new transformer into the machinery hall of the LLF

Figure 4: The cellar is lowered to its foundation next to the LLF

Figure 5: Placement of the fan controls container over the cellar

The main reason for replacement of the sting control system was the aging Moog electronics and therefore the obsolescence of this hardware. In addition to fulfilling of the existing requirements, a new functionality was required i.e.:

- Integration of the roll axis
- Improvement of the synchronization between axes pairs
- Faster network communication (TCP/IP)
- Higher measurement frequency (minimum 10 Hz)
- Averaging of measurement values
- Extensive diagnostic features

The upgrade included the installation of absolute position sensors, instead of incremental encoders, which makes the necessity to calibrate the axes positions less frequent. In addition, hydraulic valves were replaced or adapted. The sting control system (see Figure 6) is now based on an industrial PC that can control six axes, five of them directly related to the position and attitude of the sting. The sixth is a multi-purpose spare axis, usually not in use. The existing Quantum PLC, providing the control of valves and pumps, has received a new processor, and the software is adapted to the new situation. The sting hand terminal has a wireless connection, providing the required flexibility to control the sting from the test section or the testing hall, and making the operation of the sting mechanism more effective and user-friendly during the preparation of a wind tunnel test.

The replacement of the sting controls was technically complex. A first feasibility study was performed in 2003. As the search for a suitable supplier took much time, the final order for the manufacture of the system was submitted only in March 2007. The implementation of the system took place in September-October 2007 (parallel to the fan drive modernization).
The modification provides a system that incorporates today's standard technologies and is well integrated into the LLF computer infrastructure. The analog controller has been replaced by a digital controller.

Replacement LLF Flow Reference System

The flow conditions in the test section, such as dynamic pressure, air velocity and Mach number, are determined by the Flow Reference System (FRS). These reference parameters are also used for the control of the tunnel itself and cannot be measured directly. The underlying measured quantities are pressures and pressure differences, temperatures and relative humidity. Because the reference parameters are used for the conversion of raw measurement data to aerodynamic coefficients, a high degree of accuracy is very important. Although a new FRS was already delivered in 2006, the integration in the LLF infrastructure could only be performed during a longer downtime of the wind tunnel. This opportunity occurred during the replacement of the fan controls replacement in 2007.

The main reason for replacing the existing system was again the aging equipment, especially the primary pressure transducers and accompanying measuring system. It became ever more difficult to obtain spare parts for this system. Calibration and checking of the existing system became rather time-consuming and the dedicated calibration equipment itself was due for replacement. Moreover, the conversion of the FRS to a configuration, suitable for calibration of the test section or vice versa, took about two hours, mainly owing to the warming-up needed to achieve a stable condition of the equipment.

The principle of the tunnel control and reference data measurement did not change (see Figure 7). The type and number of sensors of the new system is the same as before. The major differences are the new state-of-the art pressure, temperature, and humidity sensors. The system is tuned to the low-speed regime with main differential pressure transducers of 15 kPa range. This pressure range is in fact fixed for all LLF test sections, which means that no internal valves are used. The new equipment is applicable for all four different test sections without adaptation.

The two absolute pressure sensors and the five differential pressure sensors are placed in an enclosure that is a kept at a constant temperature of 21° C. This enclosure is kept closed during the conversion to the test section calibration configuration. A second enclosure contains the thermometer and humidity equipment. The two total pressure and temperature probes in the tunnel settling chamber

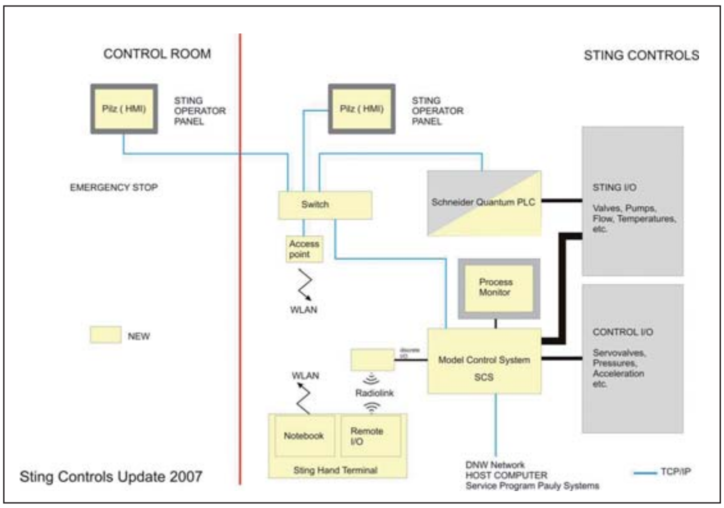

Figure 6: Schematic of the new LLF sting control system

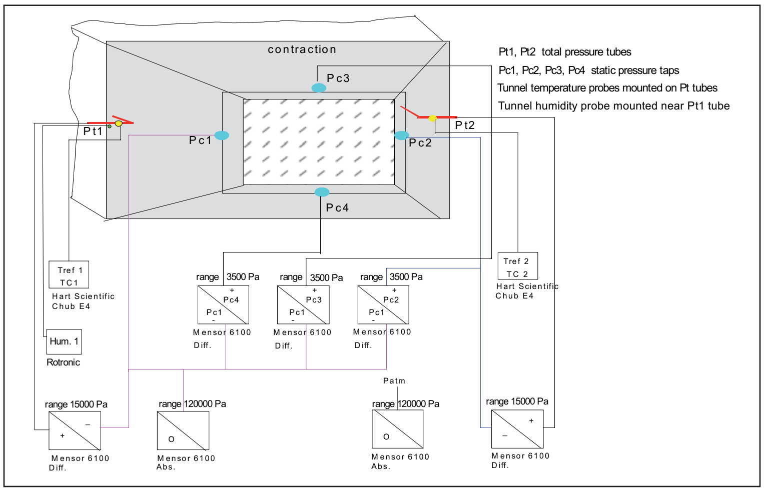

Figure 7: Schematic of the new LLF flow reference system

were replaced by new ones.
The system is designed by Scanivalve Corp. in cooperation with DNW. The pressure measurement hardware is based on Mensor pressure sensors, the accuracy of which is 0.01% full scale (including linearity, hysteresis, repeatability and temperature errors). This is far better than the old transducers. The software was designed by DNW and implemented by Scanivalve. Like in the standard static data acquisition systems at LLF, statistical outputs based on the measured data are integrated.
The FRS is a separate subsystem within the LLF data acquisition computer infrastructure, with a typical sampling rate of 20 Hz.

Before the final switch-over to the new system, it was installed parallel to the old one in order to compare the measured data of both systems under real conditions. By upgrading the system, optimal use could be made of the newest technology, for instance fully automated calibration of the equipment.
Moreover, the preparation time for test section calibrations has decreased considerably, from two hours to ten minutes. Furthermore, all the pneumatic changes for the calibration configuration can now be performed outside of the sensor box.

Unsteady Pressure Measurements on Oscillating Models

Motivation

Dynamic force measurements are performed on a regular basis at the DNW-NWB, in order to determine dynamic stability derivatives. Wind tunnel tests, which are performed to deliver dynamic results for validation and verification of unsteady computational codes, should also be able to deliver unsteady surface pressures, in addition to the balance signals. Ideally, the surface pressures should comprise model surface pressures as well as of test section wall pressures.

High- versus low speed pressure measurements

When considering dynamic pressure measurements, one has to distinguish between measurements of pressure signals with high-frequency content on the one hand and measurements of pressure signals containing low-frequency components on the other hand. In the first case (e.g. flutter or aeroelasticity investigations) the application of piezoresistive miniature pressure sensors, installed directly beneath the model's surface, is mandatory – in the second case the usage of the “standard” pressure measurement system applied in wind tunnels for steady pressure measurements is possible, if the following conditions are met:

- The geometry of the connecting tubes is known and the length of the tubes is as short as possible
- At least one surface (or "close-to-surface") mounted pressure sensor of the piezoresistive type should be available as a reference sensor
- Amplitude and phase responses are corrected either with an experimentally gained transfer function or with the transfer function resulting from an analytical solution

Pressure measurement systems available at the NWB

In 2007, NWB acquired a new Esterline Initium pressure measurement system, comprising of the central data acquisition module and 16 Digitally Temperature Compensated (DTC) differential pressure measurement modules, each equipped with 32 or 64 pressure ports.
The Initium system is capable of a total sampling rate of 20 kHz per module, leading to a maximum sampling rate of 625 Hz per pressure port (with 32 port modules).
The discrete acquisition times can be triggered individually. Currently, NWB's Initium system is triggered at each time step by the MGC+ data acquisi-

German-Dutch Wind Tunnels

tion system used for balance and Kulite signals in order to achieve the best possible synchronicity. The effect of the tubing on the dynamic pressure signals with respect to amplitude and phase is accounted for by means of a theoretical transfer function.

Pressure measurements performed at the NWB

Figure 8 depicts the most recently used set-up in the NWB, which incorporated dynamic pressure measurements. The DLR-F12 (light-weight) model is equipped with 96 pressure taps in three sections, connected by tubes of equal length to three PSI modules, located inside the model; ten additional Kulite pressure sensors were installed permanently as reference sensors.

In addition, static pressures along three lines on the test section floor and one line on the side wall, each line comprising of 24 pressure taps, were measured dynamically. To keep the tubing as short as possible, one PSI module was used for each line of pressure taps. The limited length of the electrical connections between modules and Initium requires two Initium systems to be used. The second Initium system was supplied for the tests by the DLR Institute of Aerodynamics and Flow Technology.

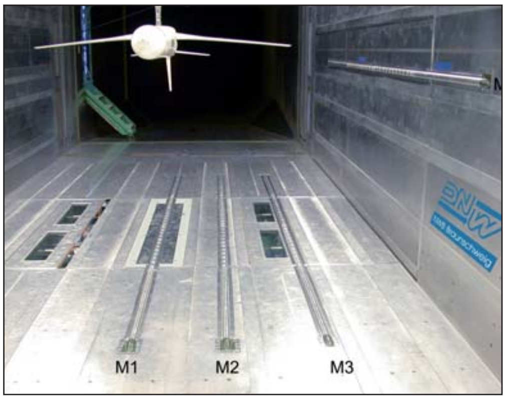

Figure 8: The DLR F12 light-weight model mounted inverted in NWB's closed test section, incorporating four rows of pressure taps for dynamic wall pressure measurements

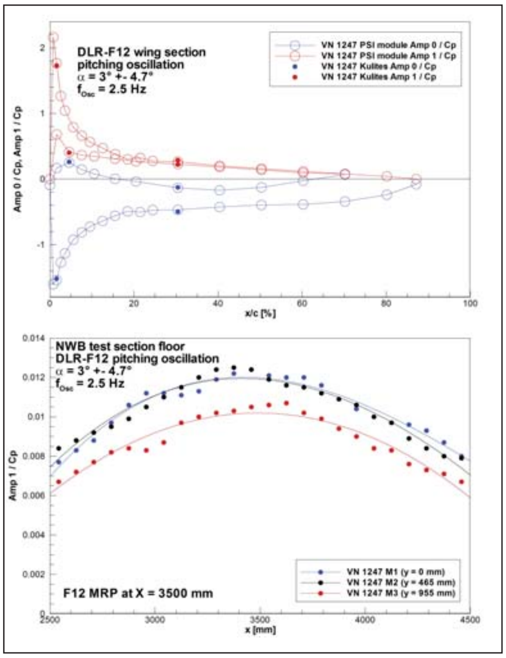

Figure 9: Typical results of unsteady pressure measurements on the DLR F12 model oscillating in pitch. The upper diagram is wing section data and the lower diagram is test section floor data

The results of the unsteady pressures on model and test section wall are exemplified in Figure 9, showing the pressure distributions belonging to a sinusoidal pitching oscillation. The upper diagram depicts the unsteady mean values and the amplitudes of the first harmonic of the wing section, while the lower diagram presents the test section floor pressure amplitudes resulting from the same pitching oscillation.
On the wing section, the very good agreement between the results of the PSI/Initium system on the one hand and the Kulite sensors on the other hand is evident.

Reconstruction of the DNW-TWG Drive System

On 11 June 2007, the compressor of the TWG failed due to fatigue in the root of one of the blades in the second of eight stages. After the failure, it was decided not only to repair the damage, but to redesign the compressor blades as well (see Figure 10). Here, not only the fatigue resistance but also the aerodynamic efficiency of the compressor was to be improved. The extent of the damage caused by the failed blade, as well as the limited availability of capacity at companies capable of performing the repairs, together resulted in a long repair period.

Encouraged by the continuous customer demand and support in the preceding period, DNW decided to utilize the compressor repair time to further concentrate other large-scale improvements and investment plans for the TWG. So the whole aerodynamic layout of the compressor will be revised and optimized and the electrical power supply will be modernized by the replacement of key components. The modernization will increase the reliability of the facility as well as the flexibility in access and change of tunnel conditions.

Qualifying the DNW-HDG for Standardized Train Tests

In anticipation of the increased usage of the HDG for train certification tests, as required by the European certification rules, as well as in response to the specifications and regulations for tests required by the manufacturing industry, DNW has proceeded to optimize and standardize the HDG hardware and operating procedures. First tests using the new approach and hardware are described in the chapter Highlights of Project Work.

Typical requirements for a train test arrangement consist of force measurements:

1. at a front car followed by a middle car and/or a dummy streamliner and/or
2. at a middle car preceded by a front car and followed by a dummy and/or
3. at an end car preceded by a front car

The two- or three-element models defined by the above requirements are to be tested on a flat ground or on a generic embankment at angles of sideslip up to β_{max} = 90°. Three-element tests can be realized at a scale of about 1:100, which corresponds to a Reynolds-number of $Re_{max} = 5 \times 10^5$ ($l_{ref\ orig.}$ = 3 m).

Figure 11 illustrates the standard test set-up in the HDG. This set-up has been optimized and developed for dedicated testing in the HDG. The model is mounted on a turntable integrated into the side-wall of the HDG. To minimize tunnel wall boundary layer effects, a splitter plate is mounted above the turntable and acts as the ground level for the train. The measured model is mounted above the splitter plate and has no contact with it. The model is connected to the external balance by two stiff and aerodynamically shielded rods at or near to the train bogies. The rod distance can be adjusted to accommodate different models. Dummy cars, which are not to be measured, are directly attached to the splitter plate.

The new set-up was first tested with an Emmen box-type six-component strain-gauge balance from the DNW stock. The stiffness of the balance and the support elements was high enough to avoid model oscillations and contact to non-metric parts. For small, reduced scale models, a smaller, reduced load range balance of the same type was purchased, in order to increase the accuracy of these types of tests (see Figure 12). By using appropriate adapters, it is simple to interchange the balances and to install the one most suitable for the actual model scale and load conditions.

The HDG allows a wide range of Reynolds-number variation by changing the model scale, the tunnel pressure, and the flow velocity. Consequently, the loads vary more than is the standard in atmospheric wind tunnels. This makes it difficult to fulfill high accuracy requirements by a single standard test set-up. Bearing that in mind, the details of the structural design were optimized and the measuring procedure was carefully adjusted, prescribing the required calibration, minimization of temperature changes, model alignment and signal filtering and integration. With the procedure as implemented, the criteria of quality like the symmetry of force and moment coefficients with respect to the sideslip angle can be guaranteed (see also Highlights of Project Work).

In addition to the measurement of forces and moments, the experimental determination of flow field details by Particle Image Velocimetry (PIV) is of particular interest in train testing. The constrained optical access, together with the high gas density in the high-pressure wind tunnel, requires special attention. In a demonstration test, the feasibility of PIV in the HDG was demonstrated. For seeding the flow, inflammable solid particles (e.g. titanium dioxide) have been used. Consequently, the HDG was equipped with special filters in all ventilation pipes, in order to prevent the fittings from being polluted by the seeding particles.

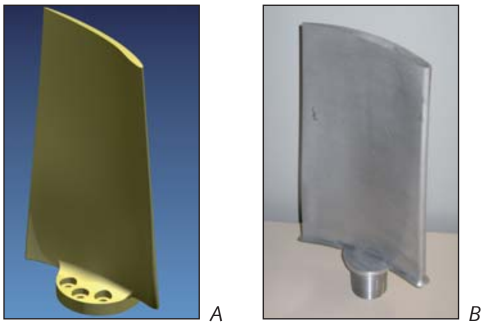

Figure 10: New shape (a) of the TWG rotor blades, designed by DLR Institutes AT and BK. The old shape (b) of the rotor blade is shown for comparison

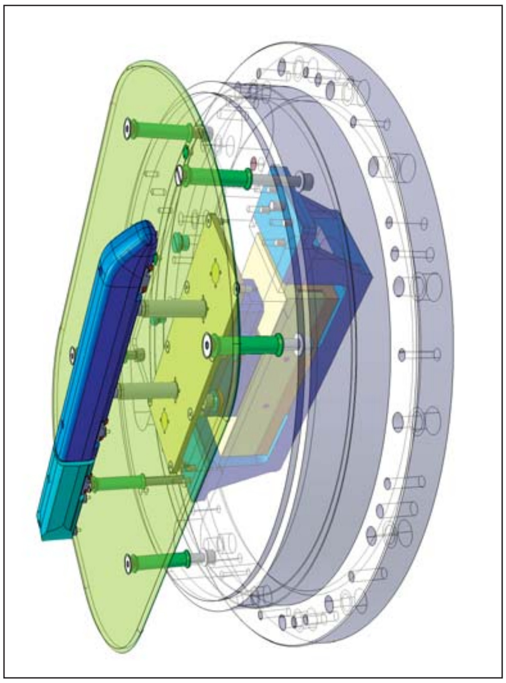

Figure 11: Schematic of the test setup in the HDG with a two-element train model, splitter plate, side-wall turntable, and external box-type balance all connected together

Figure 12: New Emmen box-type strain-gauge balance purchased for reduced-scale train tests in the HDG

Acknowledgement

All staff members who contributed to this issue of DNW's Annual Report are gratefully acknowledged. In particular, special mention is given to Alenia Aermacchi and the DLR Institutes for Aerodynamics and Technical Flows for their contributions.

Status of the Foundation

General

The Foundation DNW (German-Dutch Wind Tunnels) was jointly established in 1976 by the Dutch National Aerospace Laboratory (NLR) and the German Aerospace Center (DLR), as a non-profit organization under Dutch law. The main objective of the organization is to provide a wide spectrum of wind-tunnel tests and simulation techniques to customers from industry, government and research. DNW owns the largest low-speed wind tunnel in Europe, the LLF, and operates also the major aeronautical wind tunnels of DLR and NLR, which are fully integrated into the DNW organization. The wind tunnels operated by DNW are grouped into two Business Units "Noordoostpolder/Amsterdam" (NOP/ASD) and "Göttingen und Köln" (GUK).

The Board of DNW

The Board of the Foundation is formed from members appointed by NLR, DLR, and the German and Dutch governments. At the end of 2007, the Board consisted of:

Ir. F. Abbink, NLR, Chairman
Prof. Dr.-Ing. J. Szodruch, DLR, Vice-Chairman
Reg.Dir. A. Drechsler, German Ministry for Education and Research, BMBF
B.A.C. Droste, Netherlands Agency for Aerospace Programmes, NIVR
Drs. L.W. Esselman, R.A., NLR
Min.Dirig. K. Heyer, German Ministry of Defence, BMVg
Dipl.-Ing. H. Hüners, DLR
Ir. P.J. Keuning, Dutch Ministry of Defense
Secretary: Ms. S. Pokörn, DNW

Advisory Committee

The Advisory Committee, representing the aerospace industry and research establishments, advises the Board of DNW about the industry's long-term needs. At the end of 2007, the Advisory Committee consisted of:

Dr. B. Oskam, NLR, Chairman
M. Allongue, Eurocopter France
Dipl.-Ing. A. Flaig, Airbus Deutschland GmbH
J.C. de Jong, Stork Fokker
Prof. Dr.-Ing. J. Klenner, Airbus
Prof. Dr.-Ing. S. Levedag, DLR
Dipl.-Ing. T. Pinar, EADS Deutschland
Prof. Dr.-Ing. C.C. Rossow, DLR
L. Ruiz-Calavera, EADS CASA

The Board of Directors

DNW is managed by a Board of Directors consisting of:

Director: Dr.-Ing. G. Eitelberg, DLR
Deputy Director: Ir. C.J.J. Joosen, NLR

Organization

At the end of 2007, the permanent staff of DNW totalled 120 employees, 58 of them (including the Director) were seconded by DLR, 62 of them (including the Deputy Director) were seconded by NLR. Business Unit NOP/ASD had 89 employees and GUK 31. Two-thirds of the staff (80) were posted in the Netherlands and one-third (40) in Germany.

Publications and Presentations at Conferences

I. Philipsen, J. Zhai
Comparative Study of Strain-Gauge Balance Calibration Procedures Using the Balance Calibration Machine
45th AIAA Aerospace Sciences Meeting and Exhibit, Reno, Nevada, 08 to 11 January 2007

R. DeLoach (NASA Langley) and I. Philipsen
Stepwise Regression Analysis of MDOE Balance Calibration Data Acquired at DNW
45th AIAA Aerospace Sciences Meeting and Exhibit, Reno, Nevada, 08 to 11 January 2007

G. Eitelberg and J. Kooi
Complementing U.S. Infrastructure with DNW Capabilities
US Air Force T&E Days, Destin, Florida, 13 to 15 February 2007

G. Eitelberg
Some Critical Issues in Testing for Aircraft Technologies and the Capabilities of the German-Dutch Wind Tunnels DNW
AEROCHINA China-Europe Open Workshop, CINME, Barcelona, 25 to 27 April 2007

C.J.J. Joosen
New Components and Improvements at DNW-LLF
43rd Annual SATA Meeting, Detroit, Michigan, 10 to 14 June 2007

A. Bergmann, A.-R. Hübner (DLR)
Integrated Experimental and Numerical Research on the Aerodynamics of Unsteady Moving Aircraft
3rd International Symposium on Integrating CFD and Experiments in Aerodynamics, USAFA, Colorado Springs, Colorado, 20 to 21 June 2007

J.A. Wisse (Eindhoven University of Technology), J.W. Verkaik (Royal Netherlands Meteorological Institute), E. Willemsen
Climatological Aspects of a Wind Comfort Code
Twelfth International Conference on Wind Engineering, Cairns, Australia, 01 – 06 July 2007

E. Willemsen
Wind Tunnel Investigations to Solve Wind Related Drop Outs of a Household Waste Incineration Plant
Twelfth International Conference on Wind Engineering, Cairns, Australia, 01 – 06 July 2007

E. Willemsen
Automotive Testing in the DNW-LLF Wind Tunnel
The Aerodynamics of Heavy Vehicle Trucks, Buses and Trains, Lake Tahoe, CA, 26 to 31 August 2007

G. Eitelberg
Goals and Status of EWA
3rd EWA Joint Workshop, DNW, Göttingen, 17 to 19 September 2007

A. Bergmann, C. Kähler (Technical University Braunschweig)
Moderne Windkanalversuchstechnik zur Untersuchung instationärer Aerodynamik
Hermann Schlichting Gedächtnis-Kolloquium, Technical University Braunschweig, 28 September 2007

K.-W. Bock
Research and Development Test Spectrum of the Transonic Wind Tunnel (DNW-TWG)
108th Semiannual Meeting of STAI, Bangalore, India, 07 to 09 October 2007

T. Löser
Dynamic Testing Capabilities at DNW-NWB
8th ONERA-DLR Aerospace Symposium ODAS 2007, DNW Göttingen, 17 to 19 October 2007

G. Eitelberg
Update on Some Critical Issues in Testing for Aircraft Technologies and the Capabilities of the German-Dutch Wind Tunnels DNW
AEROCHINA 2 China-Europe Workshop, Nanjing, 22 to 24 October 2007

A. Bergmann, T. Löser, A.-R. Hübner (DLR)
Experimental and Numerical Research on the Aerodynamics of Unsteady Moving Aircraft
Publication in review journal Progress in Aerospace Science, December 2007

Organization of DNW

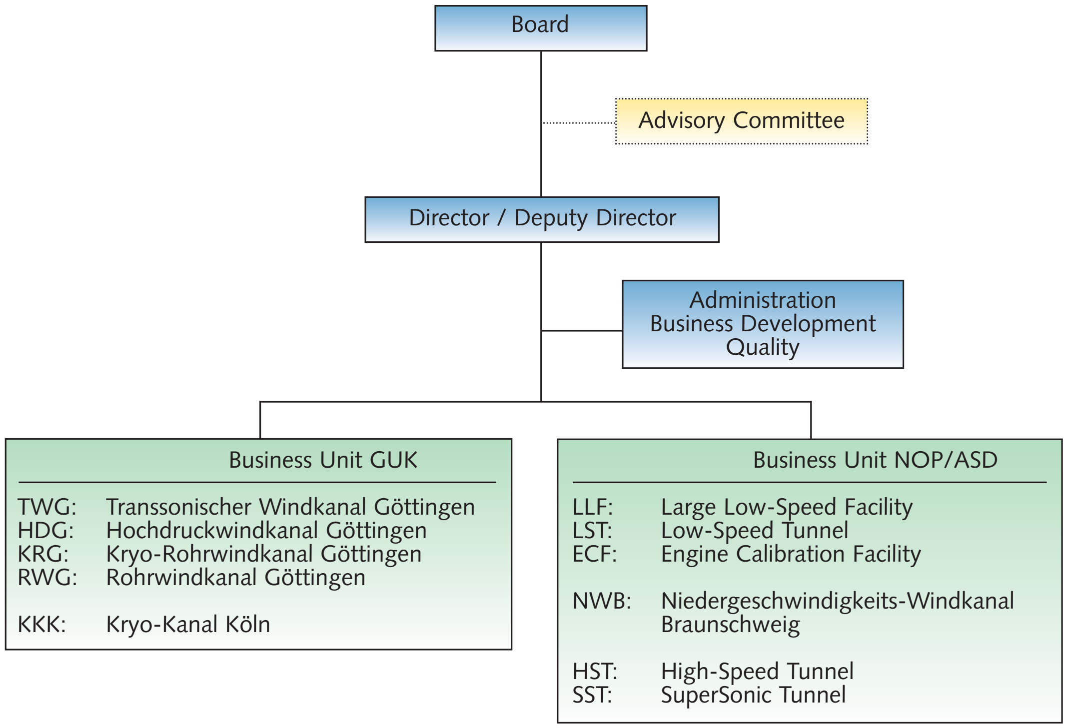

Wind Tunnels Operated by DNW

HST, SST
Anthony Fokkerweg 2
1059 CM Amsterdam
The Netherlands

Contact: G.H. Hegen
Phone: +31 527 24 8519
Fax: +31 527 24 8582
E-mail: info@dnw.aero

General Inquiry

Joost W. Kooi
Business Development

E-mail: joost.kooi@dnw.aero
Phone: +31 527 24 8505
Fax: +31 527 24 8582

NWB
Lilienthalplatz 7
38108 Braunschweig
Germany

Contact: A. Bergmann
Phone: +49 531 295 2450
Fax: +49 531 295 2829
E-mail: dnw-nwb@dnw.aero

TWG, HDG, KRG, RWG
Bunsenstraße 10
37073 Göttingen
Germany

Contact: K.-W. Bock
Phone: +49 551 709 2828
Fax: +49 551 709 2888
E-mail: dnw-guk@dnw.aero

KKK
Linder Höhe
51147 Köln
Germany

Contact: R. Rebstock
Phone: +49 2203 601 3700
Fax: +49 2203 695 961
E-mail: dnw-kkk@dnw.aero

LLF, LST, ECF
Voorsterweg 31
8316 PR Marknesse
The Netherlands

Contact G.H. Hegen
Phone: +31 527 24 8519
Fax: +31 527 24 8582
E-mail: info@dnw.aero

German-Dutch Wind Tunnels